A.A. Marelis

Energy capacity of a geothermal reservoir

The effect of conductive heat transfer recharge on reservoir lifetime at low temperature conduction regimes

TU Delft

Energy capacity of a geothermal reservoir

The effect of conductive heat transfer recharge on reservoir lifetime at low temperature conduction regimes

By

A.A. Marelis

in partial fulfilment of the requirements for the degree of

Bachelor of Science
in Applied Earth Sciences

at the Delft University of Technology,
to be defended publicly on Thursday July 20, 2017 at 16:00 PM.

Supervisor:	Dr. H. Hajibeygi, TU Delft
Co-supervisor:	Mr. T. Praditia, TU Delft
Thesis committee:	Dr. P. Vardon, TU Delft

This work was conducted at Delft Advanced Reservoir Simulation (DARSim) group.

Contents

List of figures

List of tables

Nomenclature

γ_g	Gas density gradient [kg/m^2-s^2]
γ_w	Water density gradient [kg/m^2-s^2]
λ_c	Rock thermal conductivity [W/m-K]
λ_g	Gas mobility [m^2/Pa-s]
λ_w	Water mobility [m^2/Pa-s]
λ_t	Transmissibility [kg/Pa-s]
ρ_g	Gas density [kg/m^3]
ρ_R	Rock density [kg/m^3]
ρ_w	Water density [kg/m^3]
φ	Porosity [-]
C_p	Rock specific heat capacity [J/kg-K]
C_{pw}	Water specific heat capacity [J/kg-K]
H_g	Gas enthalpy [kJ]
H_w	Water enthalpy [kJ]
p_g	Gas pressure [MPa]
p_w	Water pressure [MPa]
q	Specific volumetric source term (production or injection rate) [1/s]
q_H	Enthalpy production rate [kJ/s]
q_{HL}	Heat loss rate [1/s]
q_{hf}	Heat flow [mW/m^2]
S_g	Gas saturation [-]
S_w	Water saturation [-]
T	Temperature [^{o}C or K]
t	Time [years or sec]
U_g	Gas internal energy [J/kg]
U_w	Water internal energy [J/kg]

Abstract

The effect of conductive heat transfer recharge originating from the surrounding conduction dominated geothermal system on the geothermal reservoir lifetime has been reviewed during its development, by studying the effect of multiple reservoir and production parameters. A two dimensional (2D) finite volume implicit coupling strategy, using a direct solver method, is applied on a non-isothermal lumped-parameter model to simulate reservoir development over a period of 35 years. Two test cases are investigated, modelled after the low temperature geothermal fields of Middenmeer in The Netherlands and Soultz-sous-Forêts in France. Resulting produced thermal water temperature and thermal energy flow rate profiles are simulated with and without consideration of the geothermal system. A resolution of 200×200 equidistant structured cells is applied to cover an integrated (reservoir and surrounding) domain that extends 2 km vertically and 10 km horizontally. The reservoir domain extends 200 m vertically and 1 km horizontally, covered by a computational grid resolution of 20×20. Sensitivity analysis show that this is the best resolution that can be applied without losing simulator stability and accuracy.

Results show that the conductive heat transfer recharge originating from the surrounding geothermal system has a significant effect on reservoir lifetime by reducing temperatures after thermal drawdown up to 26.5% in the first test case and up to %22.6 in the second test case. In addition, it lead to an increase in the average annual thermal energy production, up to %12.5 and %14.3 respectively. The consideration of the conductive recharge from the surrounding domain shows a significantly increased lifetime estimate for low temperature geothermal reservoirs. Furthermore, permeability, rock thermal conductivity and (re-)injection temperature are the reservoir and production parameters that can greatly influence the reservoir lifetime.

Acknowledgements

I would like to thank Timothy Praditia for providing me with the geothermal simulator. And I would like to thank Hadi Hajibeygi for providing this Bachelor thesis subject, and reassuring me that the Petroleum Engineering master track at the Delft University of Technology is the way forward for me. This work was performed in the Advanced Reservoir Simulation (DARSim) research group.

1. Introduction

Geothermal energy is a form of energy obtained from within the Earth, originating in its core (geothermal energy, n.d.). *Geothermal* originates from the Greek words 'γη' (ge) and 'θερμός' (thermos) which mean 'Earth' and 'heat' respectively. Geothermal energy is produced by extracting the Earth's internal heat and is often referred to as 'heat-mining' (Tester et al., 2006).

Geothermal systems are often discussed using many different terms. The nomenclature provided by Grant and Bixley is adapted in this report to keep their meaning clear and consistent. Geographic names are usually assigned to areas of geothermal activity and are subsequently described as *geothermal fields*. This term is not related to the greater *geothermal system* which is responsible for creating and maintaining field activity. "The total subsurface hydrologic system associated with a geothermal field is termed a *geothermal system*" (Grant & Bixley, 2011, p. 5). A geothermal system includes the total flow path, from cold water percolating down to the heat source and heated waters migrating towards the (shallow sub)surface.
"A *geothermal reservoir* is the section of the geothermal field that is so hot and permeable that it can be economically exploited for the production of fluid or heat" (Grant and Bixley, 2011, p. 5). The geothermal reservoir, or resource, forms only a part of the geothermal field and is defined by the stored enthalpy, or thermal energy (Dickson & Fanelli, 2003).

The aim of any geothermal assessment study is on minimizing, and otherwise mitigating, the technical risks and uncertainties related to a geothermal reservoir and its potential. The principal resource risks for geothermal energy exploitation include: 1) temperature (or enthalpy), 2) depth of the resource, and 3) output and sustainability of flow from producing wells, i.e. the thermal energy that can be extracted from the resource over a certain period of time.
As many applications of geothermal energy require a minimum operating temperature (Figure 1; lindal diagram), development of geothermal systems is strongly dependent on produced water temperature. As a body containing heat cools down when heat is extracted, exploitation of geothermal reservoirs is limited by time, i.e. the reservoir lifetime. The loss of temperature in the production well over time is referred to as the thermal drawdown (Tester et al., 2006).

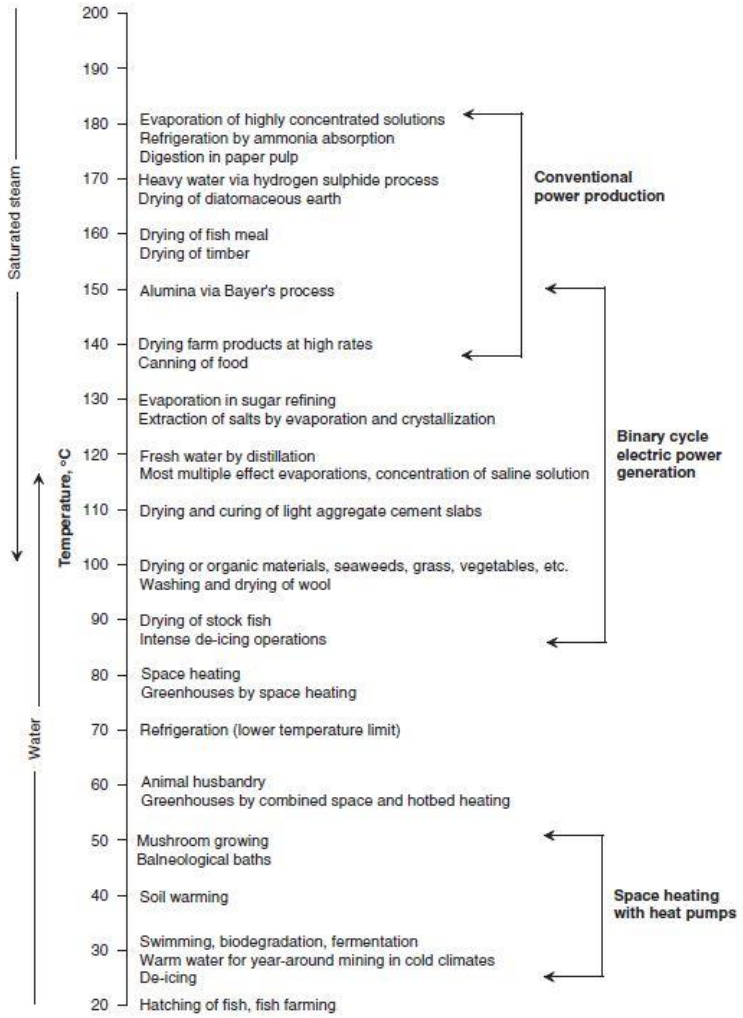

Figure 1: Illustration showing general temperature requirements of a spectrum of direct-use applications of geothermal resources. The broad temperature ranges for electric power generation from geothermal resources are indicated on the right (modified after Lindal, 1973). From Gupta & Roy, 2006.

Geothermal assessment studies focus on the reservoir, and on the response of the system to production and (re-)injection. This includes stored thermal energy in the reservoir, temperatures of produced thermal waters and natural and/or artificial recharge of fluids into the reservoir (GeothermEx, Inc. & Harvey consultants, ltd., 2012; Gehringer & Loksha, 2012). The geothermal system surrounding the reservoir often increases the reservoir lifetime by convective heat transfer into

the reservoir, when an active hydrologic circulation system is present. When this convection dominated recharge of heat is absent, heat may also be transferred into the reservoir from the surrounding hot rocks, which are part of the geothermal sytem, by means of conduction (Grant & Bixley, 2011; Tester et al., 2006).

This study aims to investigate the effect of this conductive heat transfer into the reservoir on the geothermal reservoir lifetime. By extending the domain of a geothermal reservoir simulator, the surrounding geothermal system is incorporated and reservoir development is studied with a natural recharge of heat by conductive heat transfer. Only conduction dominated geothermal systems are considered and convective heat transfer is restricted to inside the reservoir domain only, as thermal waters migrate from injection to production well. Geothermal reservoir development is simulated using various reservoir and production parameters, with and without consideration of the integrated geothermal system. Resulting produced thermal water temperatures and thermal energy flow rates over time are compared between simulations in order to determine the significance of the conductive heat transfer recharge from the surrounding geothermal system, and the influence of the various reservoir and production parameters, on reservoir lifetime.

1.1. Conduction dominated systems

Conduction dominated geothermal systems exploit latent heat encapsulated in crustal rocks. This heat originates from the average heat flux through the Earth's crust and/or from radioactive phenomena in the crustal rocks (Tester et al., 2006). This heat is transported by conduction. Although this thermal energy is present everywhere, it is usually stored at greater depth. The average continental heat flux is 65 mW/m2 (Pollack et al., 1993), but the actual value may vary from place to place over the Earth's surface. As thermal conductivity varies with different strata, conductive gradients can reach values of up to 60 ^{o}C/km. These gradients are also referred to as temperature- or geothermal gradients, with a global average of 30 ^{o}C/km. Geothermal gradients can be useful in identifying areas of anomalous heat flow, which may be associated with regions of potential geothermal resources (Grant & Bixley, 2011; Tester et al., 2006).

Examples of conduction dominated geothermal systems include:

1. Deep sedimentary aquifers: deep thermal aquifers heated by the normal geothermal gradient. Thermal waters are confined within a particular sedimentary stratum and are not part of an active circulation system (Grant & Bixley, 2011). These aquifers are most commonly exploited by a geothermal doublet. An excellent example of such a system is given by the Middenmeer geothermal field, located in the province of Noord Holland, in the Netherlands. The Middenmeer geothermal field is formed by a sedimentary thermal aquifer in the Slochteren formation (Rotliegend Sandstone). The reservoir is directly overlain by a salt layer of the Zechstein Group, followed by the Rijnland Group and the Chalk Group. The reservoir is underlain by the Limburg Group (Dinoloket, n.d.). The thermal energy extracted from the reservoir is solely used for the heating of greenhouses on an agricultural complex.

2. Enhanced (or Engineered) Geothermal Systems (EGS): comprised of rock that contains sufficient heat, but does not have sufficient intrinsic (or matrix dominated) permeability. Such hot, impermeable rock is by definition not part of the reservoir. Exploitation of such a system requires the creation (or enhancement) of permeability by hydraulic fracturing, in order to ensure fluid circulation through the rock (Grant & Bixley, 2011). Heat is extracted using a geothermal doublet, with one or more injection and/or production wells. An excellent example of such a system is given by the Soultz-sous-Forêts geothermal field in Europe. This system represents an enhanced geothermal system, although fractures are naturally present. The geothermal reservoir is located in an uplifted horst structure of granitic basement rocks/terrain. The uplifted horst structure is adjacent to the western boundary fault of the Upper Rhine Graben, which was formed by a Cenozoic rift system and is considered a major heat anomaly (Ziegler, 1994; Baillieux et al., 2013, as cited in Wanatabe et al., 2017, p. 75). The thermal energy extracted from the reservoir is used for electricity generation using a binary rankine cycle.

2. Simulation and modeling approach

The effect of the surrounding geothermal system on reservoir lifetime is investigated over a period of 35 years. Results are simulated at a time increment of 1 year. A 2 dimensional, non-isothermal lumped-parameter model is assumed. The governing equations and the simulation method are presented in this chapter, as well as model descriptions and assumptions. A finite volume implicit reservoir simulator is provided (Praditia, 2017) and simulations were performed in Matlab R2015a.

2.1. Governing equations

The geothermal reservoir simulator is based on equations derived from both mass and energy conservation laws. Hydrocarbon reservoir simulators are mainly based on the law of conservation of mass and assume isothermal conditions inside the reservoir in regards to temperature. However, as temperature variation plays an important role in geothermal reservoir simulation, the isothermal assumption is no longer valid and the law of conservation of energy must be incorporated.
The general mass conservation equation (Hajibeygi & Jenny, 2009) consists of three terms; 1) accumulation, 2) net outflow, and 3) source terms, which can be written as

$$\frac{\partial}{\partial t}\left(\phi\rho_w S_w + \phi\rho_g S_g\right) - \nabla\cdot\left[\rho_w\lambda_w(\nabla p_w - \gamma_w\nabla z) + \rho_g\lambda_g\left(\nabla p_g - \gamma_g\nabla z\right)\right] = \rho_w q_w + \rho_g q_g. \quad (1)$$

Here, $\gamma = \rho g$, where g is the gravitational acceleration. Similarly, the general energy conservation equation (Coats, 1977) is written as

$$\frac{\partial}{\partial t}\left[\left(\phi\rho_w S_w U_w + \varphi\rho_g S_g U_g\right) - (1-\phi)\left(\rho C_p\right)_R T\right] - \nabla\cdot\left[\rho_w\lambda_w H_w(\nabla p_w - \gamma_w\nabla z) + \rho_g\lambda_g H_g\left(\nabla p_g - \gamma_g\nabla z\right)\right] - \nabla\cdot(\lambda_c\nabla T) = q_{HL} + q_H, \quad (2)$$

which can be used for two phase fluid flow (if both water saturation S_w and gas saturation S_g are non-zero). Both convective and conductive terms, through enthalpies (H_w and H_g) and heat conductive coefficient λ_c, are present. Note that the heat exchange between the reservoir and the overlying and underlying strata is also considered (Coats, 1977, p. 2).

Considering a geothermal doublet, with a power plant converting the thermal waters from the production well and delivering the cooled waters to the (re-)injection well, a closed system can be assumed. This means that in terms of mass balance there is neither a source term, nor mass accumulation, and the amount of mass injected into the reservoir equals the amount of mass produced from the reservoir. Assuming furthermore that the thermal fluid is single phase water under sub-critical conditions, the mass conservation equation reduces only to net out-flux and can be simplified to single phase compressible flow (Tene, Wang and Hajibeygi, 2015) as

$$\frac{\partial}{\partial t}(\phi\rho_w) - \nabla\cdot[\rho_w\lambda_t\nabla p] = \rho_w q. \quad (3)$$

Here, λ_t is the transmissibility, which is defined as the water and/or gas mobility $\lambda_{g,w}$ times the respective density $\rho_{w,g}$ multiplied by the surface area, and divided by a unit of length. The same assumption (single-phase) is applied to the conservation of energy equation. A separate energy balance is derived which applies to the geothermal system surrounding the reservoir, thus eliminating the heat loss rate q_{HL} from the equation. For the reservoir domain, equation (2) is simplified to

$$\frac{\partial}{\partial t}\left[\phi\rho_w U_w - (1-\phi)\left(\rho C_p\right)_R T\right] - \nabla\cdot[\rho_w\lambda_t H_w\nabla \mathrm{p}\,] - \nabla\cdot(\lambda_c\nabla T) = q_H \quad \text{on} \quad \boldsymbol{\Omega}_{Res}. \quad (4)$$

Here, the unknown temperature T can be specified as the reservoir temperature T_{Res}. No convective heat transfer is considered outside the reservoir. The conductive heat source for the geothermal system is the (constant) heat flux originating from the Earth's core, q_{hf}, so for the domain surrounding the reservoir (the geothermal system outside the reservoir, i.e. $\boldsymbol{\Omega}_{Surr}$) heat is transferred only by conduction. As such, equation (2) is simplified to

$$\frac{\partial}{\partial t}\left[\left(\rho C_p\right)_R T\right] - \nabla \cdot (\lambda_c \nabla T) = q_{hf} \qquad \text{on} \quad \boldsymbol{\Omega}_{Surr} \tag{5}$$

Here, the unknown temperature T can be specified as the surrounding temperature T_{Surr}. Equations (3), (4), and (5) are non-linear because of the pressure and temperature dependency of fluid density, and internal energy and enthalpy of the water. The linearization schemes used for the energy conservation equation and equations (4) and (5) are given below

$$U_w = U_{ws} + C_{pw,s}(T - T_s), \tag{6}$$

where the water internal energy is calculated using the water internal energy at saturation condition, U_{ws} of 420000 J/kg, and the water specific heat at saturation condition, $C_{pw,s}$ of 4200 J/kg-K. Moreover, water enthalpy reads

$$H_w = U_w + \frac{p}{\rho_w}, \tag{7}$$

which can be calculated from the internal energy and is dependent on pressure and density.

2.2. System of linear equations and direct solver

The geothermal reservoir simulator uses a finite volume implicit (backward Euler) coupling strategy to solve for pressure first, followed by temperature. The mass and energy conservation equations for the next time step (n+1) are calculated using equations (8), for the mass balance, and (9) for the energy balance

$$\frac{\varphi^{n+1}\rho_w^{n+1} - \varphi^n \rho_w^n}{\Delta t} - \nabla.(\rho_w^{n+1}\lambda_t \nabla p^{n+1}) = \rho_w^{n+1} q, \tag{8}$$

$$\begin{cases} \dfrac{\phi\rho_w^{n+1}U_w^{n+1} - \phi\rho_w^n U_w^n - (1-\phi)\left(\rho C_p\right)_{R,Res}\left(T_{Res}^{n+1} - T_{Res}^n\right)}{\Delta t} - \nabla \cdot \left[\rho_w^{n+1}\lambda_t H_w^{n+1}\nabla p^{n+1}\right] - \nabla \cdot (\lambda_t \nabla T_{Res}^{n+1}) = q_H^{n+1} & \text{on} \quad \boldsymbol{\Omega}_{Res} \\ \dfrac{\left(\rho C_p\right)_{R,Surr}\left(T_{Surr}^{n+1} - T_{Surr}^n\right)}{\Delta t} - \nabla \cdot (\lambda_t \nabla T_{Surr}^{n+1}) = q_{hf} & \text{on} \quad \boldsymbol{\Omega}_{Surr} \end{cases}, \tag{9}$$

Newton's linearization lemma is used to approximate pressure and/or temperature dependent properties denoted by $\xi(p,T)$, i.e.

$$\xi^{n+1}(p,T) \approx \xi^{\nu+1} = \xi^{\nu} + \left.\frac{\partial \xi}{\partial (p,T)}\right| [(p,T)^{\nu+1} - (p,T)^{\nu}), \tag{10}$$

which, e.g. for fluid density reads

$$\rho_w^{n+1} \approx \rho_w^{\nu+1} = \rho_w^{\nu} + \left.\frac{\partial \rho_w}{\partial p}\right|^{\nu+1}, \tag{11}$$

with $(p^{\nu+1} - p^{\nu}) = \partial p^{\nu+1}$. The pressure and/or temperature dependent properties are then solved at $p^{\nu+1}$ and $T^{\nu+1}$ (the superscripts (ν) and $(\nu+1)$ denote the old and new Newton–Raphson iteration levels, respectively) in order to approximate p^{n+1} and T^{n+1}, the pressure and temperature values at the next time step. Substituting the Newton's linearization of the different properties into their respective balances results in a system of linear equations for pressure and temperature, expressed at p^{ν} and T^{ν}.

$$A_p^{\nu} \cdot p^{\nu+1} = f_p^{\nu}, \tag{12}$$

and

$$A_T^{\nu} \cdot T^{\nu+1} = f_T^{\nu}. \quad (13)$$

In this project, these linear systems are solved for $p^{\nu+1}$ and $T^{\nu+1}$ using a direct solver (Matlab backslash operator). The solutions for $p^{\nu+1}$ and $T^{\nu+1}$ are used to update $p^{\nu} = p^{\nu+1}$ and $T^{\nu} = T^{\nu+1}$ iteratively until the residual falls below a certain tolerance value (inner loop, for both temperature and pressure). A second iteration is applied to make sure the dependencies for both equations are taken into account, i.e. update the $p^{\nu+1}$ and $T^{\nu+1}$ values (outer loop).

2.4. Model Setup

The 2 dimensional model for the geothermal system consists of 200 by 200 cells and covers a depth interval of 2 km and a lateral extent of 10 km. The reservoir domain consists of 20 by 20 cells covering a reservoir thickness of 200 m and a lateral extent of 1000 m. The resulting cell dimensions are 10 m by 50 m, with the lateral length being 5 times greater than the vertical length. The strata over- and underlying the reservoir have a total thickness of 900 m (90 cells above and below the reservoir) and the strata laterally adjacent to the reservoir equals reservoir thickness.
Subsurface temperatures are distributed according to depth, from the top to bottom model surface, using a geothermal gradient and an annual average surface temperature. This temperature distribution is continued through the reservoir domain of the model. An average reservoir pressure is applied according to the pore pressure at the average depth of the reservoir.
Heat is extracted by a single geothermal doublet with a spacing of 900 m between the injection and production well. The injection well is perforated at 5 evenly spaced depth intervals covering the total reservoir thickness. The production well is perforated at 4 evenly spaced intervals located halfway the injection well perforation intervals, as illustrated in figure 2.
The parameters that will be investigated include 1) permeability, 2) porosity, 3) rock thermal conductivity, 4) rock specific heat capacity, and 5) injection temperature.

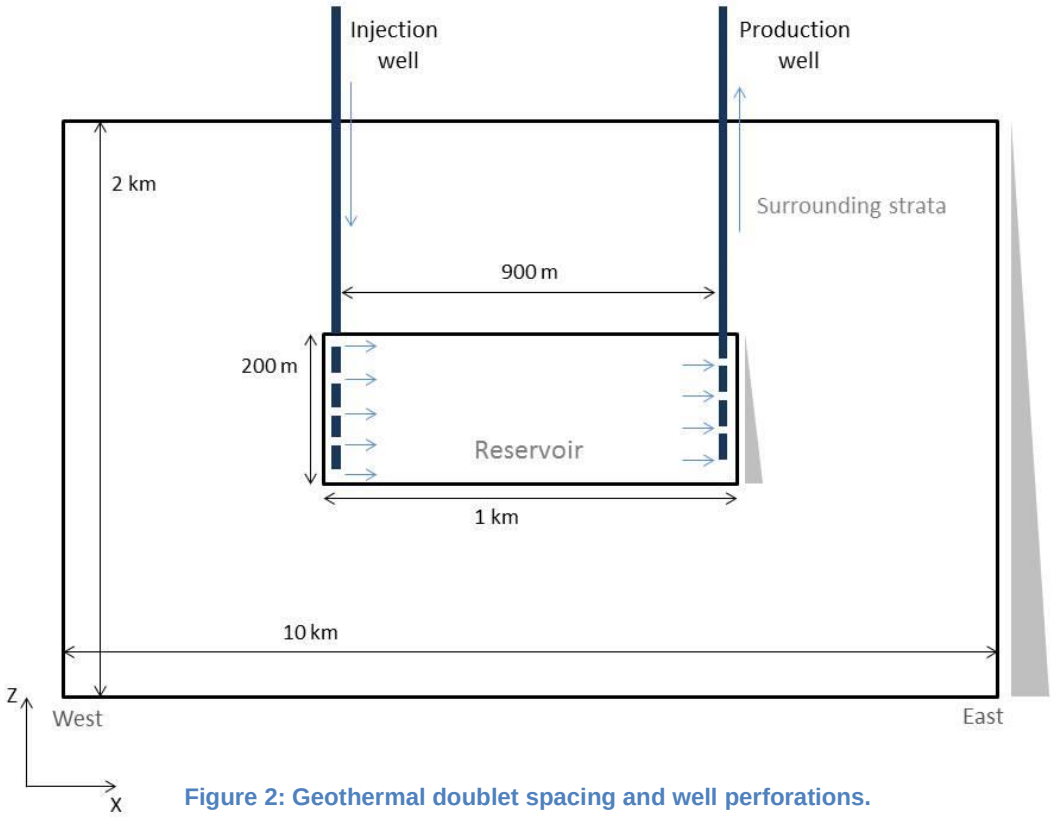

Figure 2: Geothermal doublet spacing and well perforations.

The simulation parameters, iterations and convergence tolerances are listed in table 1.

Simulation parameter	Value
Simulation time [years]	35
Time step [years]	1
Number of time steps	36
Maximum allowable iterations inner loop - Pressure - Temperature	 100 100
Maximum allowable iterations outer loop	100
Convergence tolerance inner loop - Pressure - Temperature	 10^{-5} 10^{-5}
Convergence tolerance outer loop	10^{-3}

Table 1: Key simulation parameters.

2.4.1. Model assumptions

As mentioned in the introduction, the model assumes both conductive and convective heat transfer inside the reservoir domain, and only conductive heat transfer in the domain surrounding the reservoir. The lumped-parameter model assumes both homogeneity and heterogeneity of rock properties in the simulation domain for the geothermal system, and isotropy of rock and reservoir parameters. A non-isothermal initial temperature distribution is applied.

Furthermore, no loss of volume of thermal fluid due to the density contrast generated by heat extraction in the surface power plant is assumed (Wanatabe et al., 2016). In addition, no heat loss at the well interface in the reservoir, and no heat loss in the well itself are assumed.

2.4.2. Boundary conditions

The reservoir is bounded by impermeable boundaries, and thus a no-flow boundary condition is assumed for all reservoir boundaries. This means there is no convective heat transfer between the reservoir and its surroundings. Conductive heat transfer, however, can take place across reservoir boundaries. Neumann boundary conditions are used to implement production and injection rates. For the domain surrounding the reservoir, a Dirichlet boundary condition of constant temperature is applied to the boundary at the top model surface (northern boundary). This temperature is determined by extrapolation of a geothermal gradient to the depth of the top model surface. A Neumann boundary condition of constant heat flux is applied to the boundary at the bottom model surface (southern boundary) and is determined according to the local or global average heat flow.

3. Test cases

In order to make a selection in the wide variety of parameters influencing geothermal reservoirs and their respective systems, 2 test cases are considered; 1) the Middenmeer geothermal field, and 2) the Soultz-sous-Forêts geothermal field. Modeling after these existing geothermal fields reduces parameters variability like initial pressure- and temperature distribution, and the thermal influx into the system.

2.2.2. Test Case 1

The first test case is modelled after the geothermal system of Middenmeer, assuming heterogeneity in the simulation domain and isotropy of rock and reservoir parameters. Figure 3 shows the top of the reservoir is present at a depth of 2 km, the reservoir is about 200 m thick in the area and has an average temperature of approximately 90 ^{o}C, as a gradient of 38 ^{o}C/km applies. An annual average surface temperature of 10.6 ^{o}C is assumed for the Middenmeer area (Middenmeer, North Holland Monthly Climate Average, Netherlands, n.d.). The average initial reservoir pressure is set at 21 MPa, injection pressure equals 1.5 times the initial reservoir pressure and water thermal conductivity equals 0.6 W/m-K. The constant heat flux q_{hf} into the system matches the average continental heat flux of 65 mW/m^2 (Pollack et al., 1993).

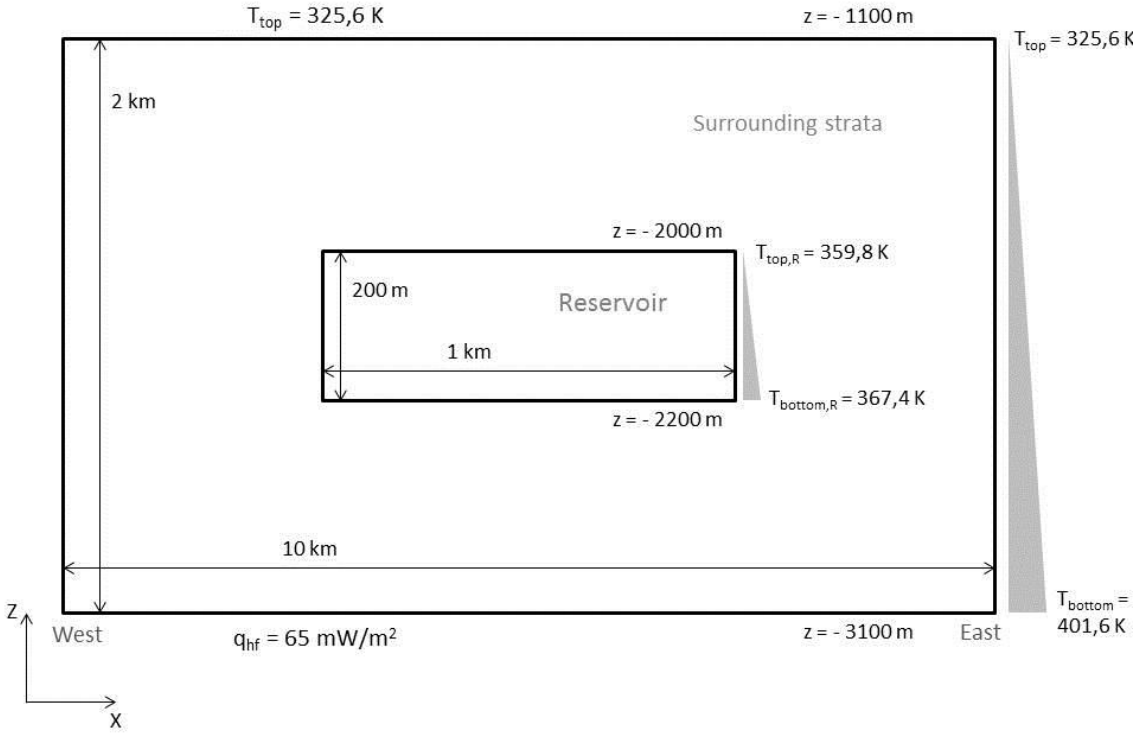

Figure 3: In-situ boundary conditions test case 1; Middenmeer geothermal system. The vertical temperature distribution is illustrated on the right hand side of the figure.

The parameters that will be investigated in test case 1 include: 1) porosity, 2) permeability, and 3) injection temperature. Rock properties such as density, thermal conductivity and specific heat capacity are fixed with the modelled geology. An overview of these rock property distributions is given in figure 4.

Figure 4: Rock thermal properties of test case 1; Middenmeer geothermal system. Density in kg/m^3, thermal conductivity in W/m-K and specific heat capacity in J/kg-K. Values are compiled from Daniilidis et al., 2016 and Eppelbaum et al., 2014.

The investigated parameters and their (variable) values are listed in table 2.

Parameter	Value			Source
	(1)	(2)	(3)	
Porosity [-]	0.1	0.15	0.2	Daniilidis, Doddema & Herber, 2016
Permeability [mD]	15	45	120	Daniilidis, Doddema & Herber, 2016
Injection temperature [^{o}C]	20	35	50	Estimated

Table 1: Variable model parameters. Sources are listed in table.

2.2.3. Test Case 2

The second test case is modelled after the geothermal system of Soultz-sous-Forêts in France, assuming homogeneity in the simulation domain and isotropy of rock and reservoir parameters. Figure 5 shows the top of the reservoir is located at a depth of 3600 m. The reservoir has a an average temperature of approximately 120 ^{o}C and reservoir thickness is set to 200 m. An average geothermal gradient of 30 ^{o}C/km is applied (Wanatabe et al., 2017) and an average annual surface temperature of 11.3 ^{o}C is assumed (Soultz-Sous-Forets, Alsace 14 Day Weather Forecast, France, n.d.).
The average initial reservoir pressure is set at 37 MPa, injection pressure equals 1.5 times the initial reservoir pressure, and water thermal conductivity equals 0.6 W/m-K The constant heat flux q_{hf} into the system equals 140 mW/m^2 (Pribnow & Clauser, 2000).

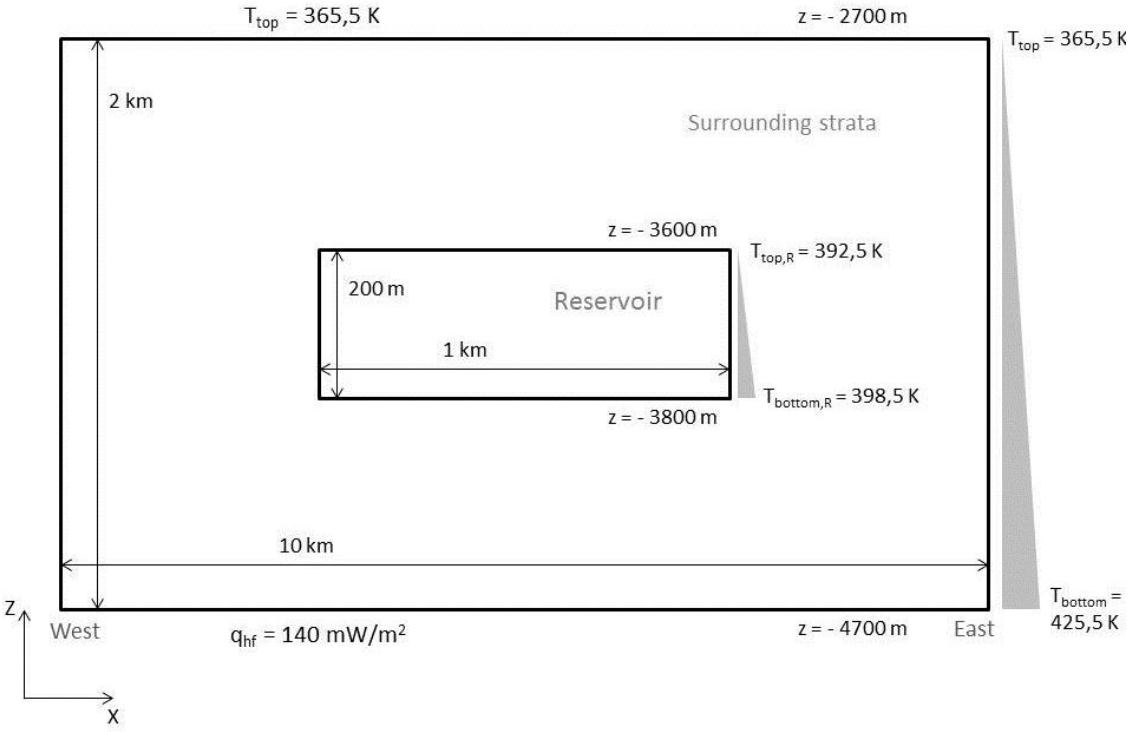

Figure 5: In-situ boundary conditions test case 2; Soultz-sous-Forêts geothermal system. The vertical temperature distribution is illustrated on the right hand side of the figure.

Permeability of the granitic body is enhanced through intense faulting and fracturing, as the permeability in the fractures is estimated to exceed values of 10 mD (Blacher et al., 2003, as cited in Wanatabe et al., 2017, p. 77). The matrix dominated permeability, however, does not exceed 0.1 mD. Since test case 2 represents an enhanced geothermal system, fracture dominated permeability must be assumed and therefore a fixed value of 10 mD is set for the model permeability. The porosity of the model is set to 1%.
The parameters that will be investigated in test case 2 include; 1) rock thermal conductivity, 2) rock specific heat capacity, and 3) injection temperature. The investigated parameters and their (variable) values are listed in table 3.

Parameter	Value			Source
	(1)	**(2)**	**(3)**	
Thermal conductivity [W/m-K]	2	3	4	Wanatabe et al., 2017
Specific heat capacity [J/kg-K]	750	850	950	Wanatabe et al., 2017
Injection temperature [^{o}C]	30	50	70	Estimated

Table 3: Variable model parameters. Sources are listed in table and apply only to value (2).

4. Results

The results of the simulation are plotted at each perforation depth of the production well, showing the effect of the varying values of the parameter under consideration for both temperature and thermal energy, over time. The term 'WS' in the legend of the figures applies to the solid lines and stands for 'With Surroundings'. It indicates the temperature, or energy, profiles of the simulations where the geothermal system is incorporated. The term 'RO' applies to the dashed lines and stands for 'Reservoir Only'. It indicates the respective profiles of the simulations where only the reservoir is considered.

4.1. Test case 1

The simulation results of test case 1 (Middenmeer geothermal field) are shown in figure 6 to figure 8 for the water temperatures from the production well over time and figure 9 to figure 11 show the thermal energy profiles of the production well. The annual average thermal energy extracted from the field is presented in table 4. The relative decrease in thermal drawdown over a period of 35 years is quantified in table 5.

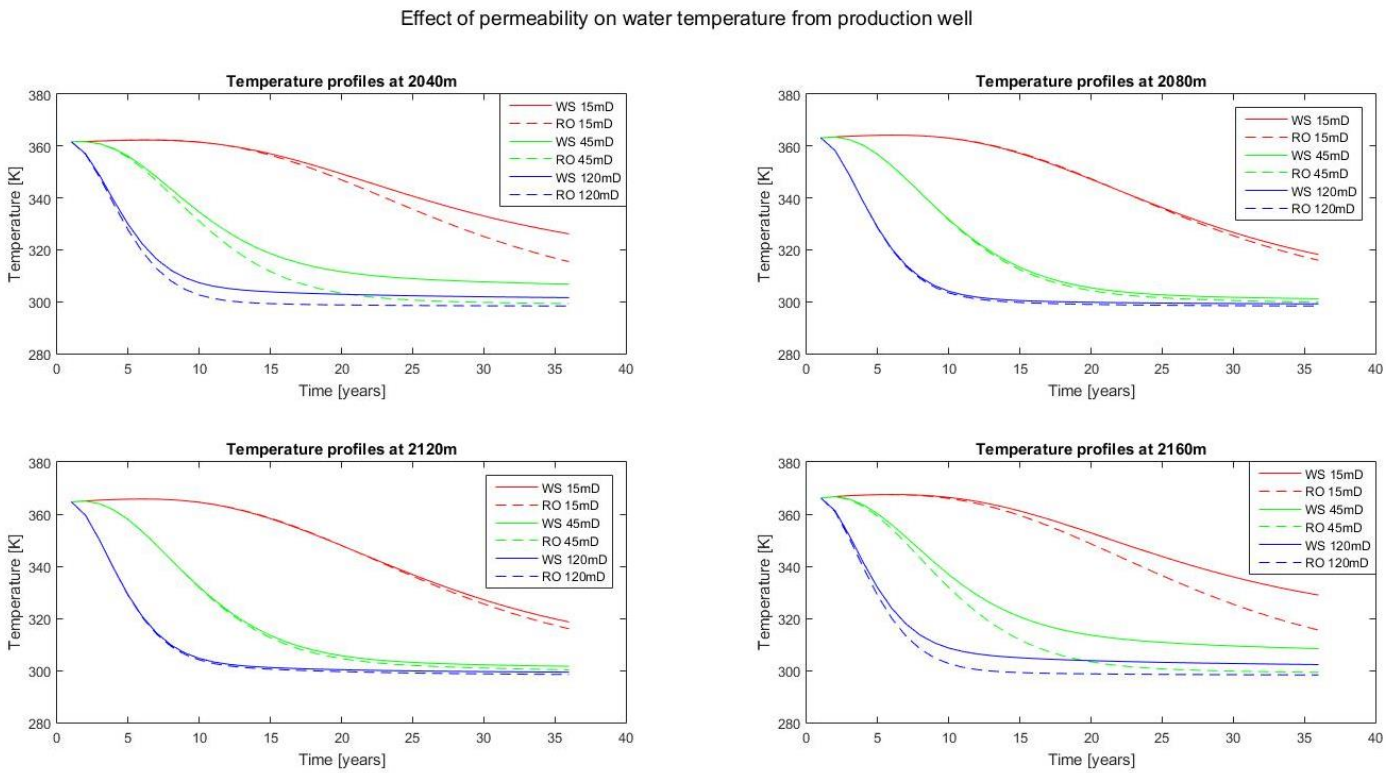

Figure 6: The effect of permeability on water temperature from production well. Remaining parameters from table 2 are fixed, i.e. 1) 15% porosity, and 2) 20 ^{o}C injection temperature.

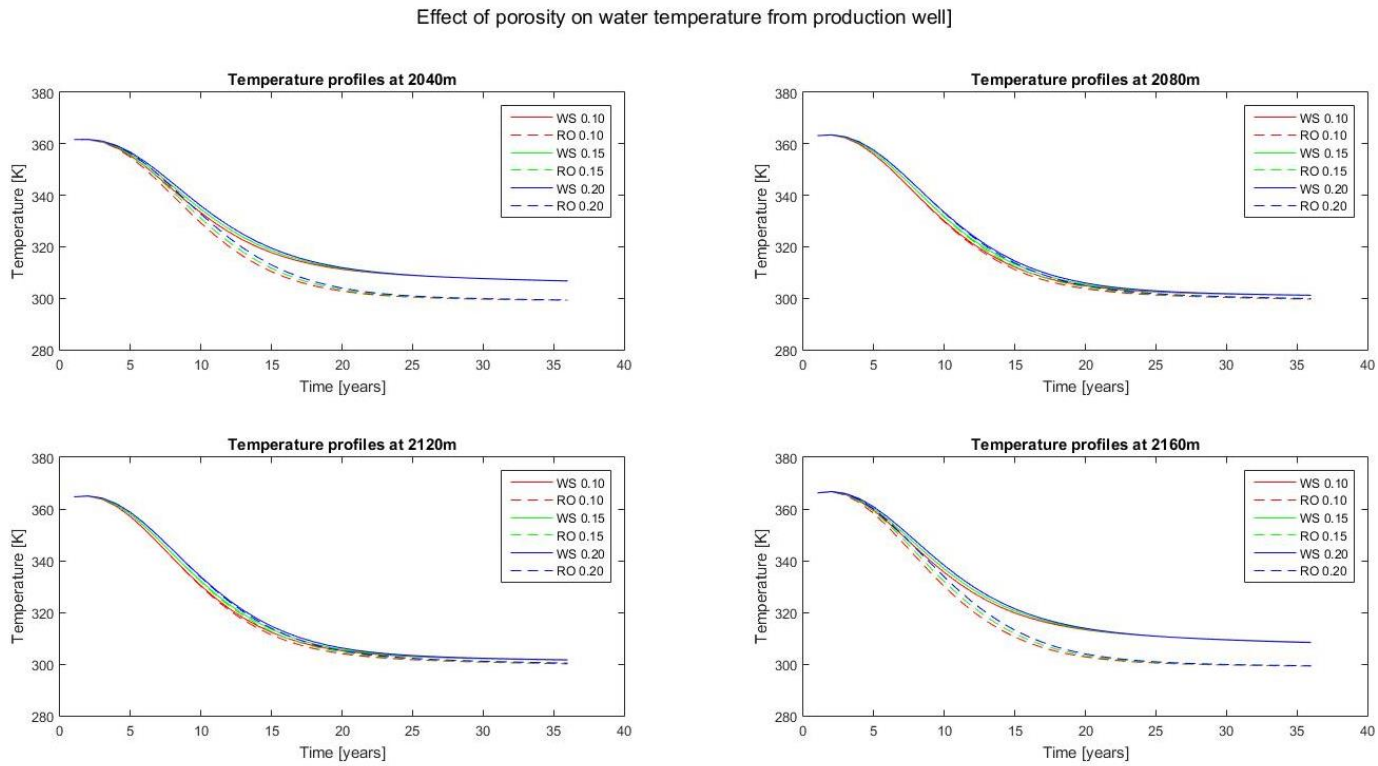

Figure 7: The effect of porosity on water temperature from production well. Remaining parameters from table 2 are fixed, i.e. 1) 45 mD permeability, and 2) 20 ^{o}C injection temperature.

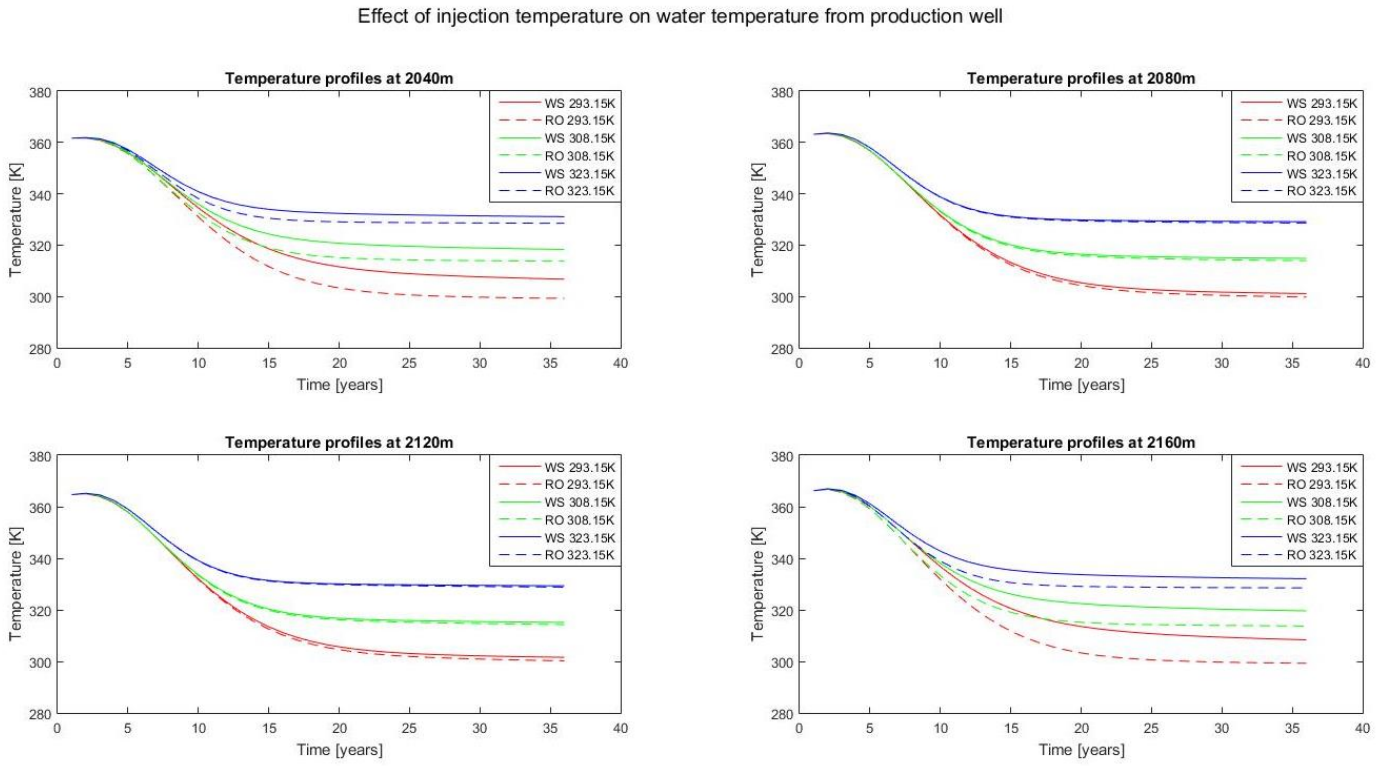

Figure 8: The effect of injection temperature on water temperature from production well. Remaining parameters from table 2 are fixed, i.e. 1) 15% porosity, and 2) 45 mD permeability.

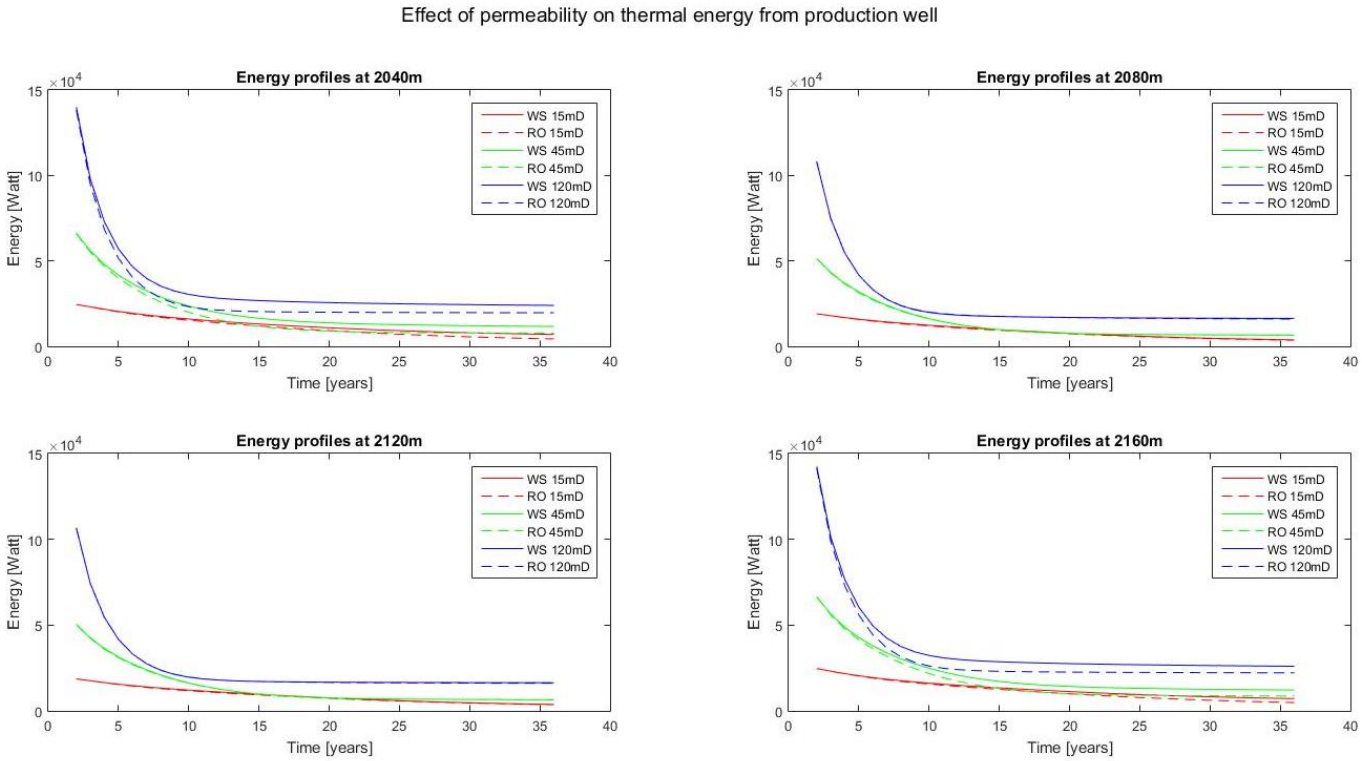

Figure 9: The effect of permeability on thermal energy from production well. Remaining parameters from table 2 are fixed, i.e. 1) 15% porosity, and 2) 20 ^{o}C injection temperature.

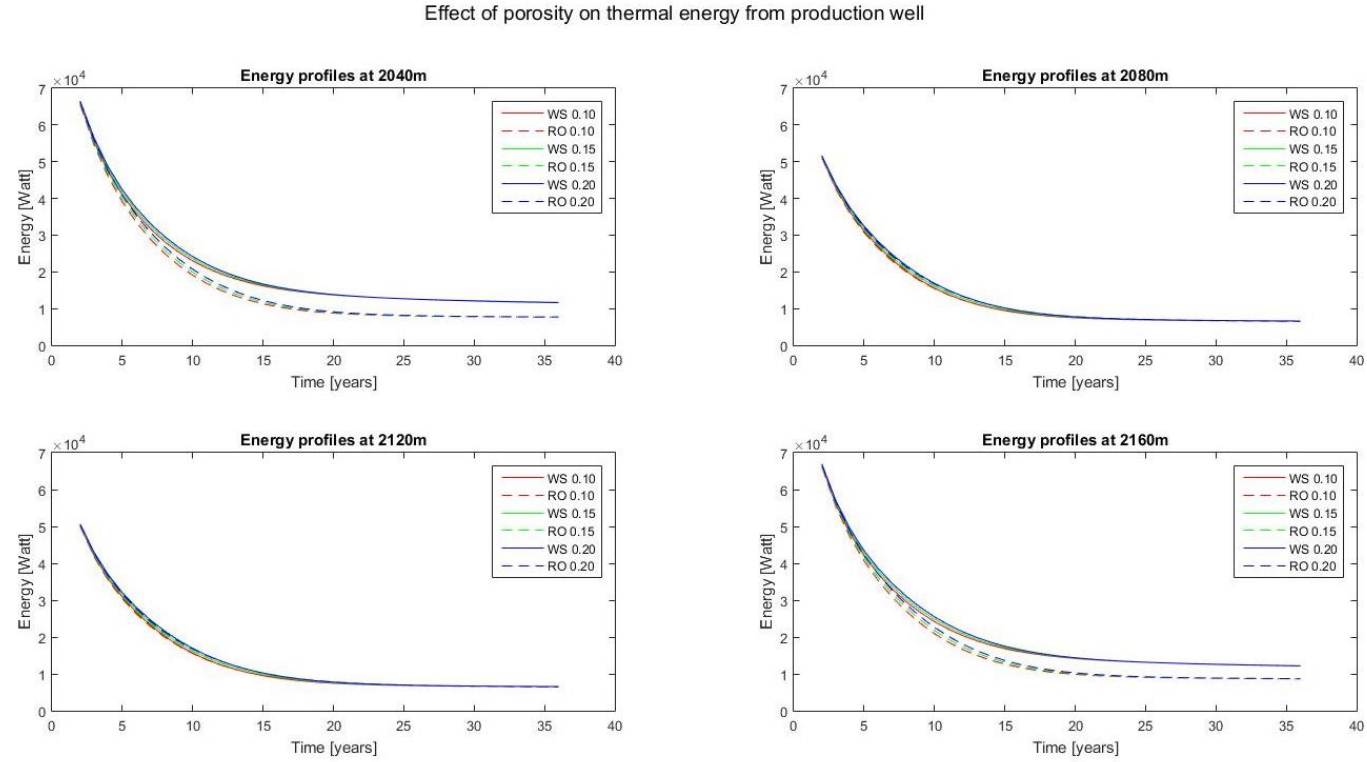

Figure 10: The effect of porosity on thermal energy from production well. Remaining parameters from table 2 are fixed, i.e. 1) 45 mD permeability, and 2) 20 ^{o}C injection temperature.

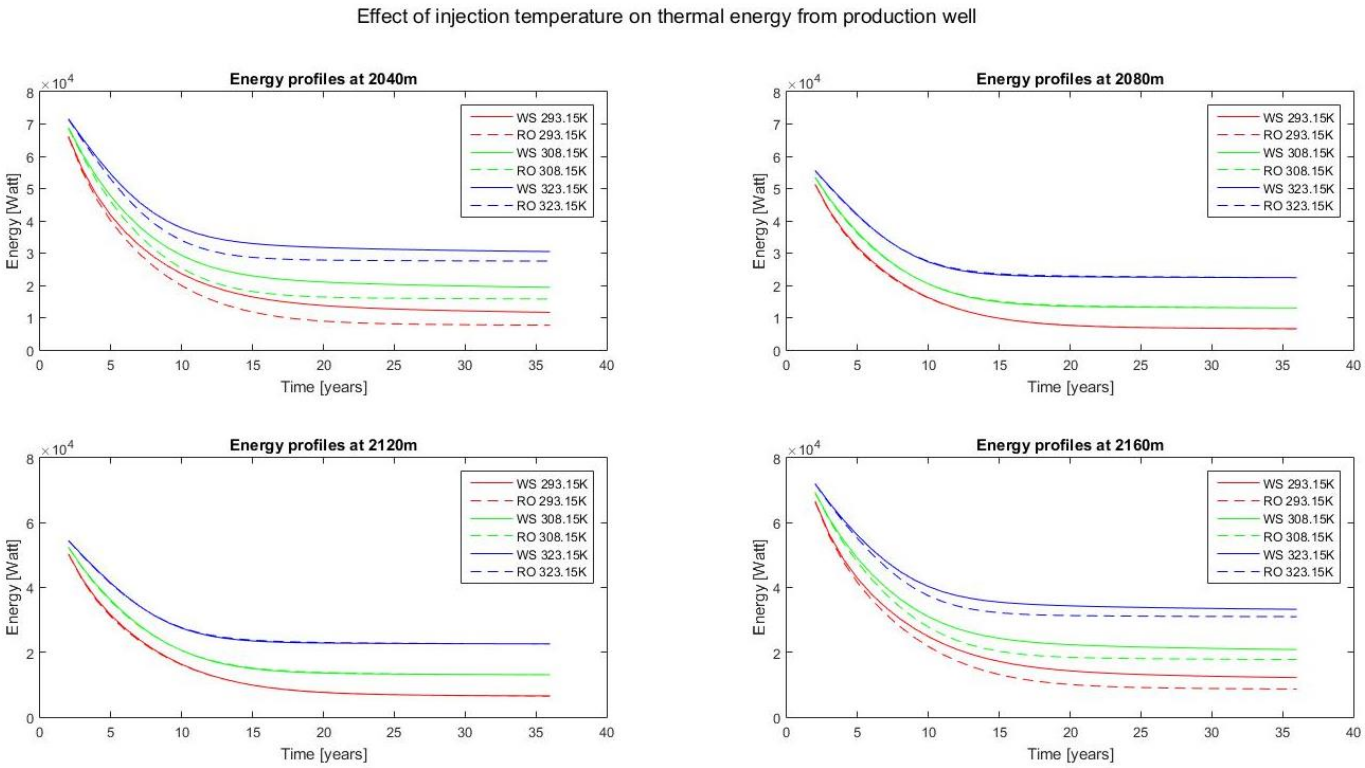

Figure 11: The effect of injection temperature on thermal energy from production well. Remaining parameters from table 2 are fixed, i.e. 1) 15% porosity, and 2) 45 mD permeability.

Parameter and value	Annual average thermal energy produced [kilowatt]		Relative increase [%]
	With Surroundings	***Reservoir Only***	
Permeability [mD]			
15	43.61	40.41	7.9
45	69.45	62.11	11.8
120	119.71	109.33	9.5
Porosity [%]			
10	68.43	60.85	12.5
15	69.45	62.11	11.8
20	70.45	63.37	11.2
Injection Temperature [^{o}C] (/ [K])			
20	69.45	62.11	11.8
35	94.44	87.66	7.7
50	130.73	125.21	4.4

Table 4: Annual average thermal energy extracted by production well according to varying values of investigated parameters from test case 1. The thermal energy is in kilowatts. The final column states the relative increase in annual average thermal energy production with the integrated surrounding geothermal system.

Parameter (and values)	Depth [m]	$T_{initial}$ [K]	T_{system} [K]	$T_{reservoir}$ [K]	ΔT [K]	Reduction thermal drawdown [%]
Permeability [mD]						
15	2040	361.65	326.15	315.43	10.72	23.2
	2080	363.17	318.18	315.96	2.22	4.7
	2120	364.69	318.59	315.96	2.63	5.4
	2160	366.21	328.93	315.48	13.45	26.5
45	2040	361.65	306.74	299.26	7.48	12.0
	2080	363.17	301.14	299.76	1.38	2.2
	2120	364.69	301.58	300.21	1.37	2.1
	2160	366.21	308.36	299.26	9.1	13.6
120	2040	361.65	301.55	298.32	3.23	5.1
	2080	363.17	299.15	298.33	0.82	1.3
	2120	364.69	299.35	298.45	0.9	1.4
	2160	366.21	302.25	298.27	6.98	5.9
Porosity [%]						
10	2040	361.65	306.77	299.19	7.58	12.1
	2080	363.17	301.11	299.64	1.47	2.3
	2120	364.69	301.53	300.06	1.47	2.3
	2160	366.21	308.42	299.20	9.22	13.8
15	2040	361.65	306.74	299.26	7.48	12.0
	2080	363.17	301.14	299.76	1.38	2.2
	2120	364.69	301.58	300.21	1.37	2.1
	2160	366.21	308.36	299.26	9.10	13.6
20	2040	361.65	306.69	299.33	7.36	11.8
	2080	363.17	301.17	299.87	1.30	2.1
	2120	364.69	301.63	300.36	1.27	2.0
	2160	366.21	308.28	299.33	8.95	13.4
Injection Temperature [K]						
293.15	2040	361.65	306.74	299.26	7.48	12.0
	2080	363.17	301.14	299.76	1.38	2.2
	2120	364.69	301.58	300.21	1.37	2.1
	2160	366.21	308.36	299.26	9.10	13.6
308.15	2040	361.65	318.33	313.74	4.59	9.6
	2080	363.17	314.85	313.96	0.89	1.8
	2120	364.69	315.14	314.29	0.85	1.7
	2160	366.21	319.59	313.73	5.86	11.2
323.15	2040	361.65	331.08	328.51	2.57	7.8
	2080	363.17	329.13	328.60	0.53	1.5
	2120	364.69	329.32	328.79	0.53	1.5
	2160	366.21	332.07	328.50	3.57	9.5

Table 5: Initial reservoir temperatures and produced water temperatures after 35 years quantified for the simulations of test case 1 considering only the geothermal reservoir and the integrated geothermal system. Temperature differences after 35 years of development are given, as well as the relative decrease in thermal drawdown over a period of 35 years.

4.2. Test case 2

The simulation results of test case 2 (Soultz-sous-Forêts geothermal field) are shown in figure 12 to figure 14 for the water temperatures from the production well over time and figure 15 to figure 17 show the thermal energy profiles of the production well. The annual average thermal energy extracted from the field is presented in table 6. The relative decrease in thermal drawdown over a period of 35 years is quantified in table 7.

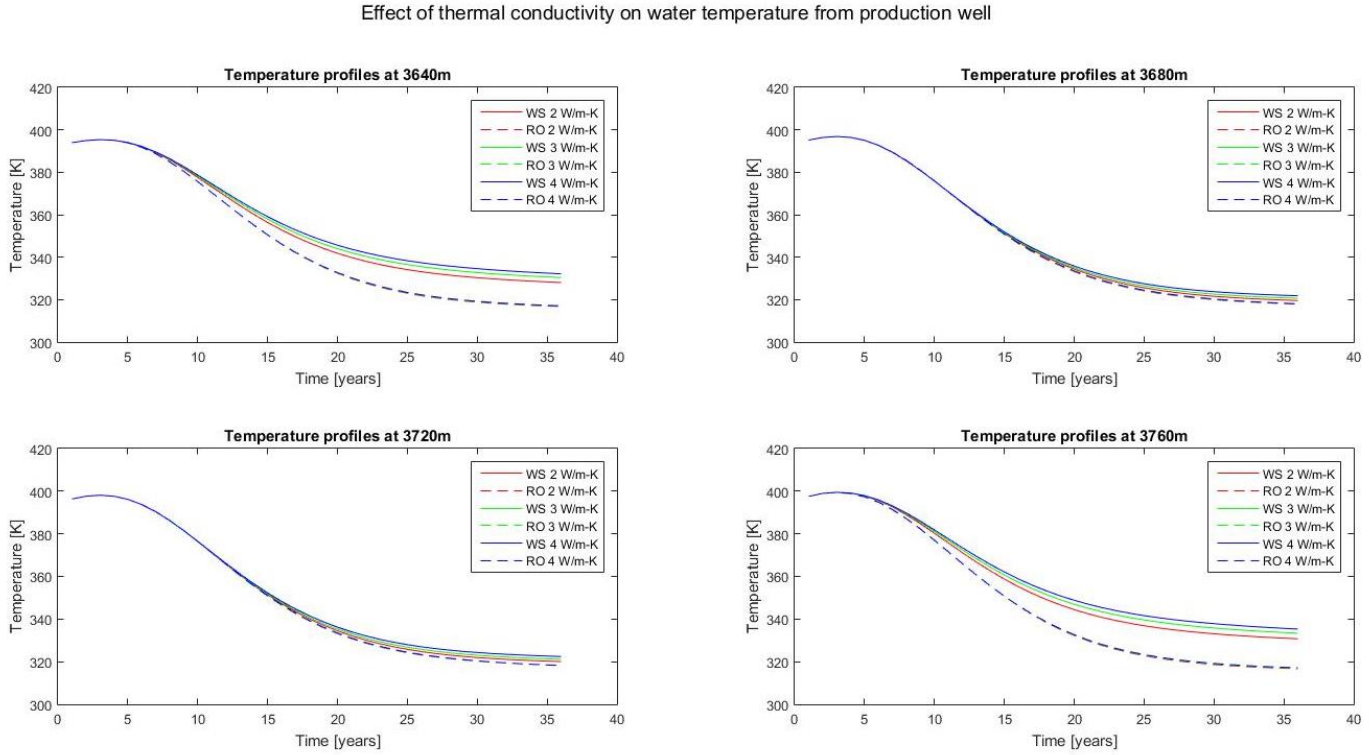

Figure 12: The effect of rock thermal conductivity on water temperature from production well. Remaining parameters from table 3 are fixed, i.e. 1) 850 J/kg-K rock specific heat capacity, and 2) 30 ^{o}C injection temperature.

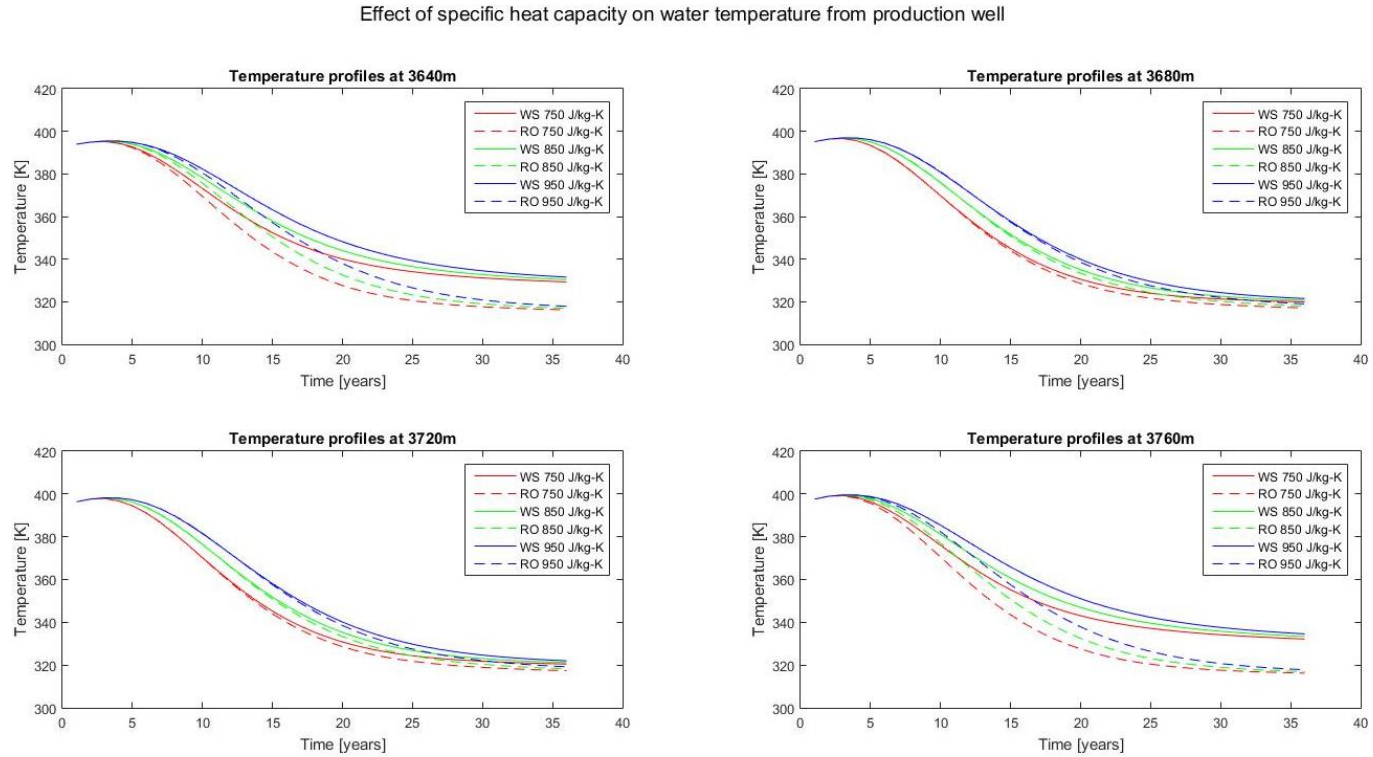

Figure 13: The effect of rock specific heat capacity on water temperature from production well. Remaining parameters from table 3 are fixed, i.e. 1) 3 W/m-K rock thermal conductivity, and 2) 30 ^{o}C injection temperature.

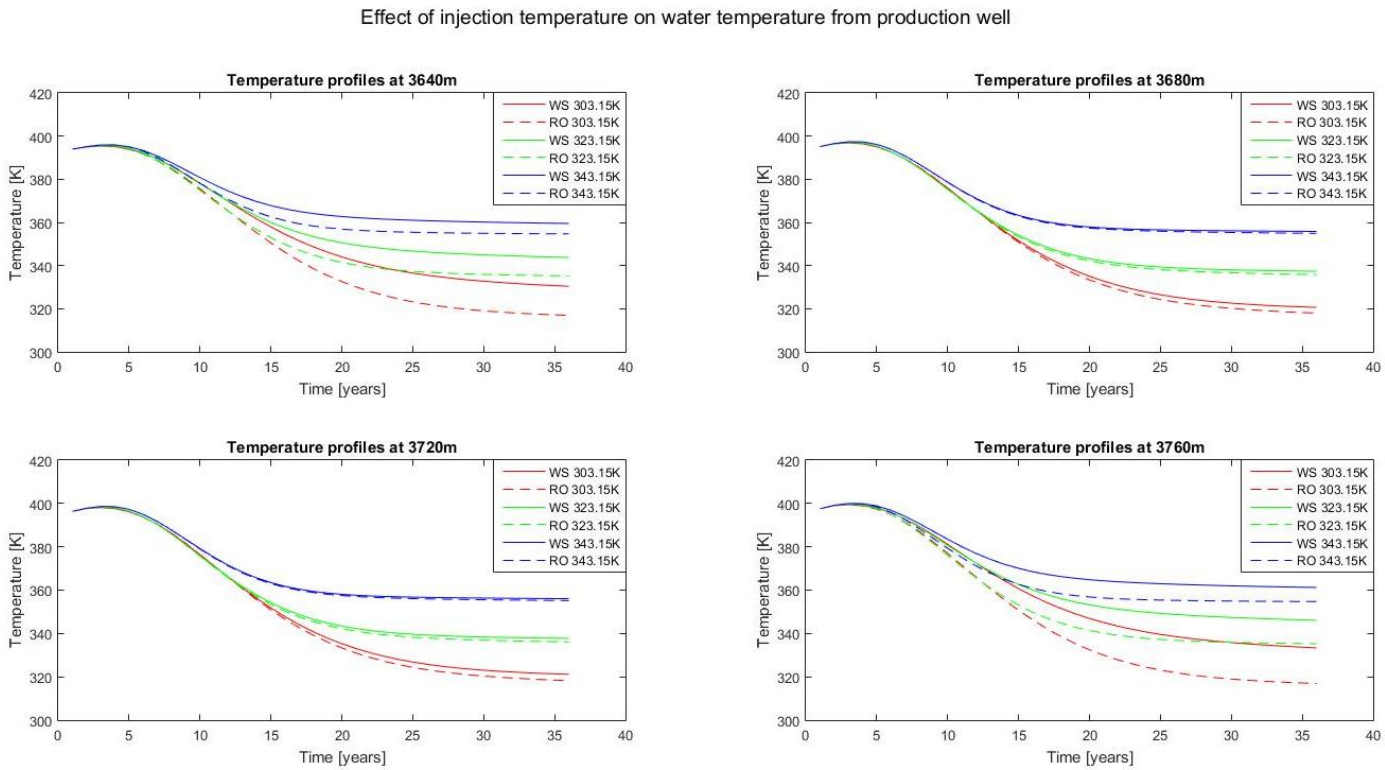

Figure 14: The effect of injection temperature on water temperature from production well. Remaining parameters from table 3 are fixed, i.e. 1) 3 W/m-k rock thermal conductivity, and 2) 850 J/kg-K rock specific heat capacity.

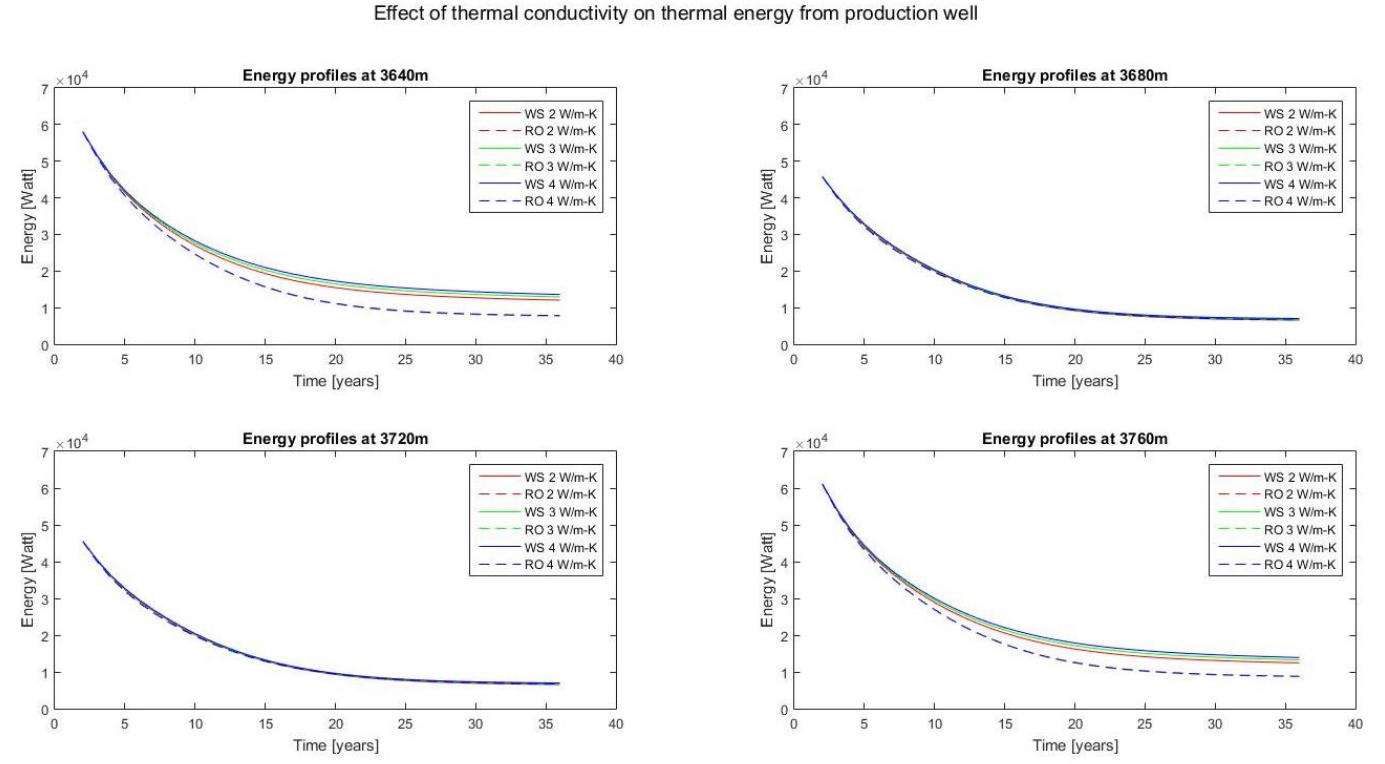

Figure 15: The effect of rock thermal conductivity on thermal energy from production well. Remaining parameters from table 3 are fixed, i.e. 1) 850 J/kg-K rock specific heat capacity, and 2) 30 ^{o}C injection temperature.

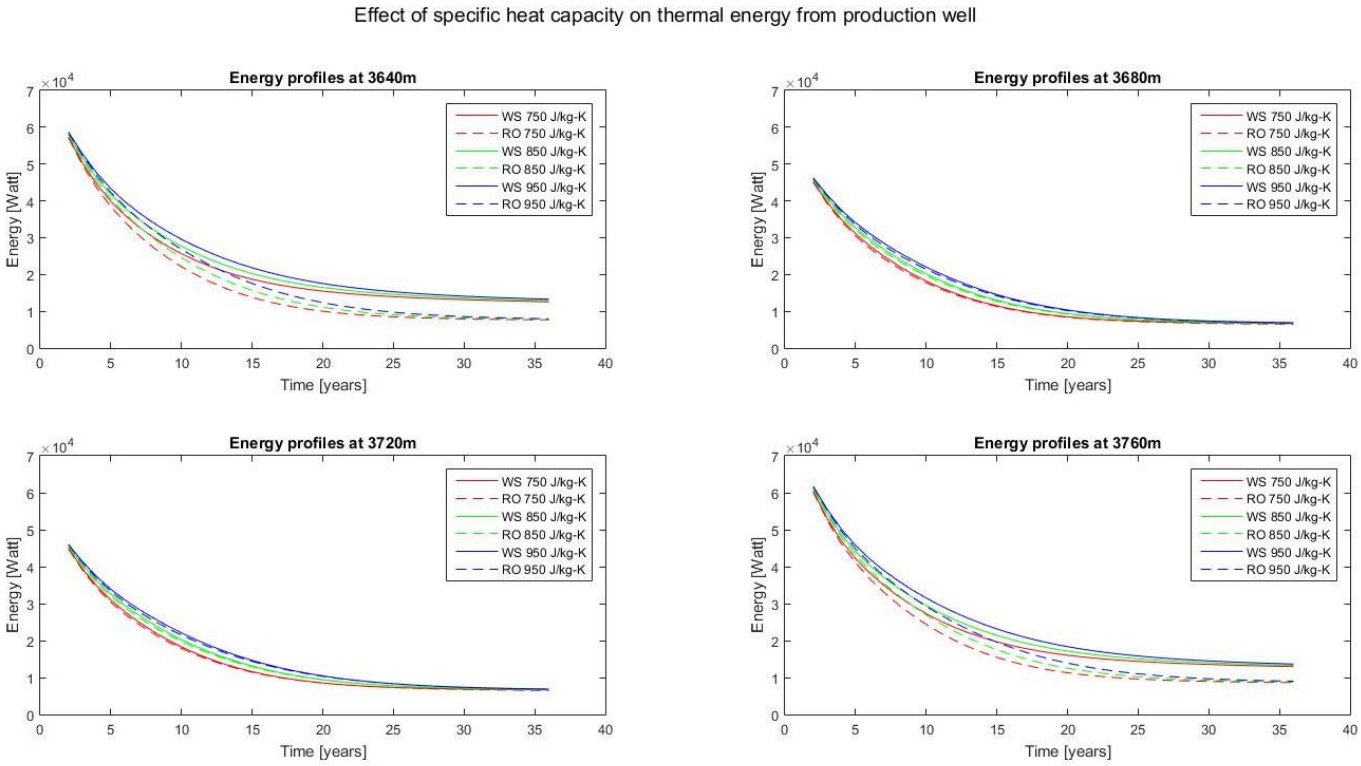

Figure 16: The effect of rock specific heat capacity on thermal energy from production well. Remaining parameters from table 3 are fixed, i.e. 1) 3 W/m-K rock thermal conductivity, and 2) 30 ^{o}C injection temperature.

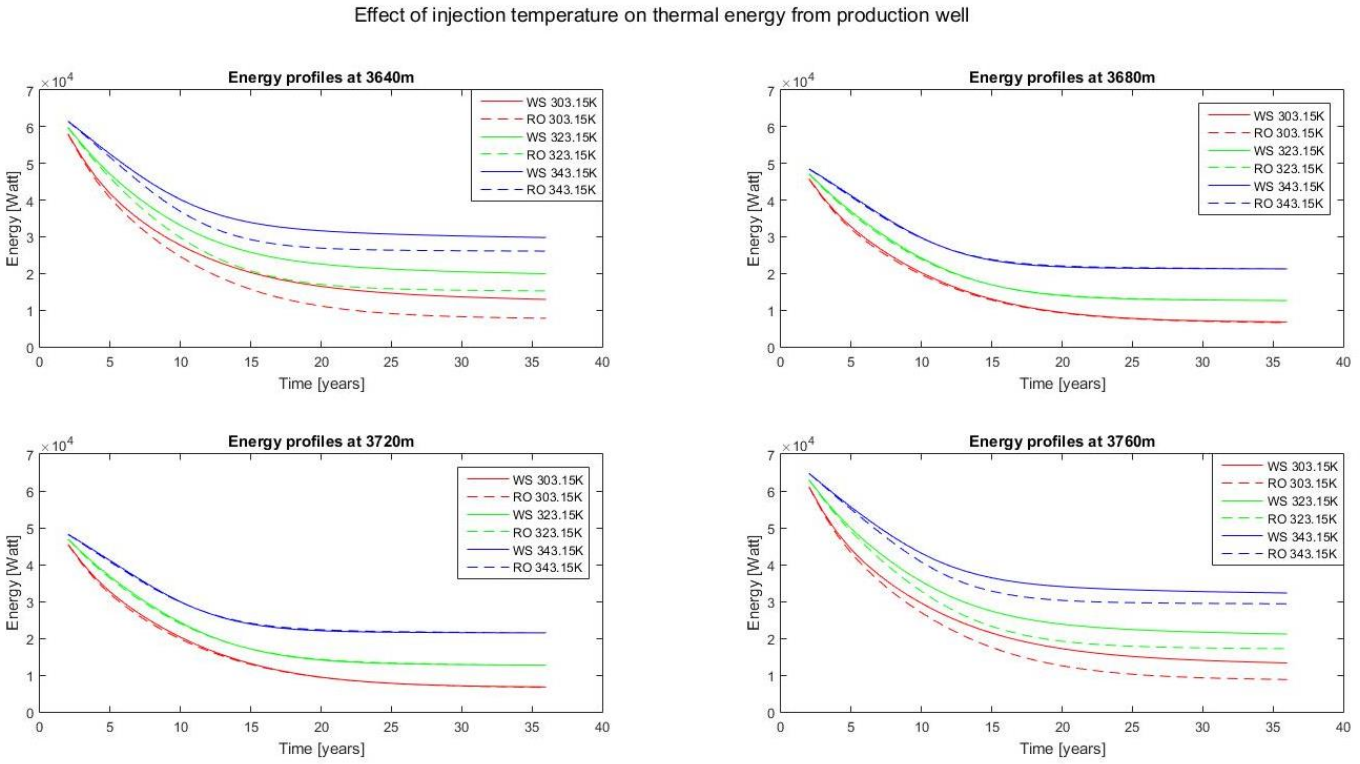

Figure 17: The effect of injection temperature on thermal energy from production well. Remaining parameters from table 3 are fixed, i.e. 1) 3 W/m-k rock thermal conductivity, and 2) 850 J/kg-K rock specific heat capacity.

Parameter and value	Annual average thermal energy produced [kilowatt]		Relative increase [%]
	With Surroundings	***Reservoir Only***	
Rock thermal conductivity [W/m-K]			
2	74.52	67.88	9.782
3	76.37	68.06	12.21
4	77.95	68.23	14.25
Rock specific heat capacity [J/kg-K]			
750	72.09	63.63	13.3
850	76.37	68.06	12.21
950	80.54	72.42	11.21
Injection Temperature [^{o}C] (/ [K])			
30	76.37	68.06	12.21
50	98.02	90.26	8.597
70	129.09	122.84	5.088

Table 6: Annual average thermal energy extracted by production well according to varying values of investigated parameters from test case 2. The thermal energy is in kilowatts. The final column states the relative increase in annual average thermal energy production with the integrated surrounding geothermal system

Parameter (and values)	Depth [m]	$T_{initial}$ [K]	T_{system} [K]	$T_{reservoir}$ [K]	ΔT [K]	Reduction thermal drawdown [%]
Rock thermal conductivity [W/m-K]						
2	3640	393.95	328.07	316.76	11.31	14.7
	3680	395.15	319.56	317.84	1.72	2.2
	3720	396.35	320.06	318.27	1.79	2.3
	3760	397.55	330.74	316.68	14.06	17.4
3	3640	393.95	330.39	316.93	13.46	17.5
	3680	395.15	320.62	317.96	2.66	3.5
	3720	396.35	321.16	318.21	2.95	3.8
	3760	397.55	333.35	316.93	16.42	20.4
4	3640	393.95	332.15	317.07	15.08	19.6
	3680	395.15	321.82	318.03	3.79	4.9
	3720	396.35	322.42	318.18	4.24	5.4
	3760	397.55	335.31	317.12	18.19	22.6
Rock specific heat capacity [J/kg-K]						
750	3640	393.95	329.30	316.20	13.1	16.9
	3680	395.15	319.92	317.08	2.84	3.6
	3720	396.35	320.46	317.36	3.1	3.9
	3760	397.55	332.17	316.23	15.94	19.6
850	3640	393.95	330.39	316.93	13.46	17.5
	3680	395.15	320.62	317.96	2.66	3.5
	3720	396.35	321.16	318.21	2.95	3.8
	3760	397.55	333.35	316.93	16.42	20.4
950	3640	393.95	331.54	317.84	13.7	18
	3680	395.15	321.48	318.97	2.51	3.3
	3720	396.35	321.99	319.18	2.81	3.6
	3760	397.55	334.57	317.80	16.77	21
Injection Temperature [K]						
303.15	3640	393.95	330.39	316.93	13.46	17.5
	3680	395.15	320.62	317.96	2.66	3.5
	3720	396.35	321.16	318.21	2.95	3.8
	3760	397.55	333.35	316.93	16.42	20.4
323.15	3640	393.95	343.77	335.24	8.53	14.5
	3680	395.15	337.35	335.81	1.54	2.6
	3720	396.35	337.73	336.09	1.64	2.7
	3760	397.55	346.08	335.27	10.81	17.4
343.15	3640	393.95	359.51	354.69	4.82	12.3
	3680	395.15	355.82	354.95	0.87	2.2
	3720	396.35	356.06	355.17	0.89	2.2
	3760	397.55	361.22	354.71	6.51	15.2

Table 7: Initial reservoir temperatures and produced water temperatures after 35 years quantified for the simulations of test case 2 considering only the geothermal reservoir and the integrated geothermal system. Temperature differences after 35 years of development are given, as well as the relative decrease in thermal drawdown over a period of 35 years.

5. Discussion

5.1. Sensitivity analysis

This section will address the uncertainties related to estimates and computations made in this study, how these uncertainties have been dealt with and what their consequences are.

5.1.1. Simulator resolution

Incorporating the geothermal system in a geothermal reservoir simulator requires extending/expanding the simulation scale. While the thickness of the geothermal reservoir (where the fluid dynamics happen) generally does not exceed a couple of hundred meters, a geothermal system can encompass several kilometers easily, especially in regards to depth. As a consequence, the number of cells used for a simulation on such a scale increases significantly when cell dimensions are kept constant, as well as computational time. In order to reduce the number of cells, one could opt for increasing the cell dimensions, possibly decreasing simulator accuracy and stability, but also decreasing computational time. A more profound approach would be development of a multiscale method for this integrated system (Praditia, 2017). The temperature profiles of a general test case, combining test cases 1 and 2, are plotted in figure 18 for six different number of cells used in the simulation, while the system dimensions are kept constant; cell dimensions, thus, also vary (table 8). Figure 18 and figure 19 (thermal energy profiles) show the effect of resolution on simulator results. An important note is computation time increased from less than a minute for 50 by 50 cells, to almost 45 minutes for 500 by 500 cells.

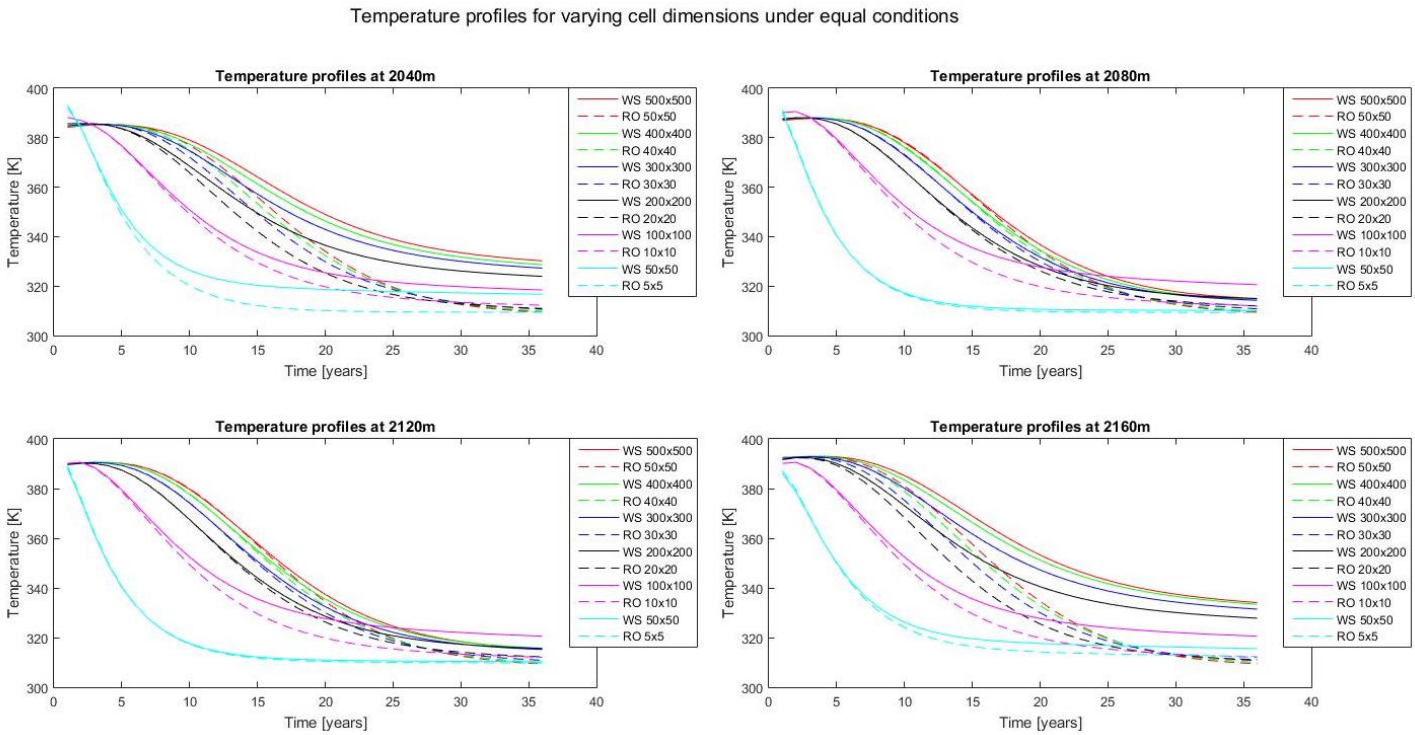

Figure 18: The effect of different cell numbers, and cell dimensions, on simulation results illustrated by temperature profiles of a generalised test case. Model dimensions and parameters are kept constant.

From figure 18 and figure 19 it becomes clear that the differences between results decrease with increasing cell number (or decreasing cell dimension), thus making the simulator more accurate. In terms of temperature (figure 18); temperature profiles of the 500, 400, 300 and 200 cell numbers tend to converge as the geothermal reservoir cools down to injection temperature. The 100 and 50 cell number profiles form an exception to this as the corresponding cell dimension Δy approaches the spacing between two successive perforations in the production well, thus lumping together all properties in between. This is clearly illustrated in the energy profiles (figure 19) of the perforations at 2040m and 2160m, where the 100 and 50 cell number profiles give completely different results at the 2040m and 2160m perforations.

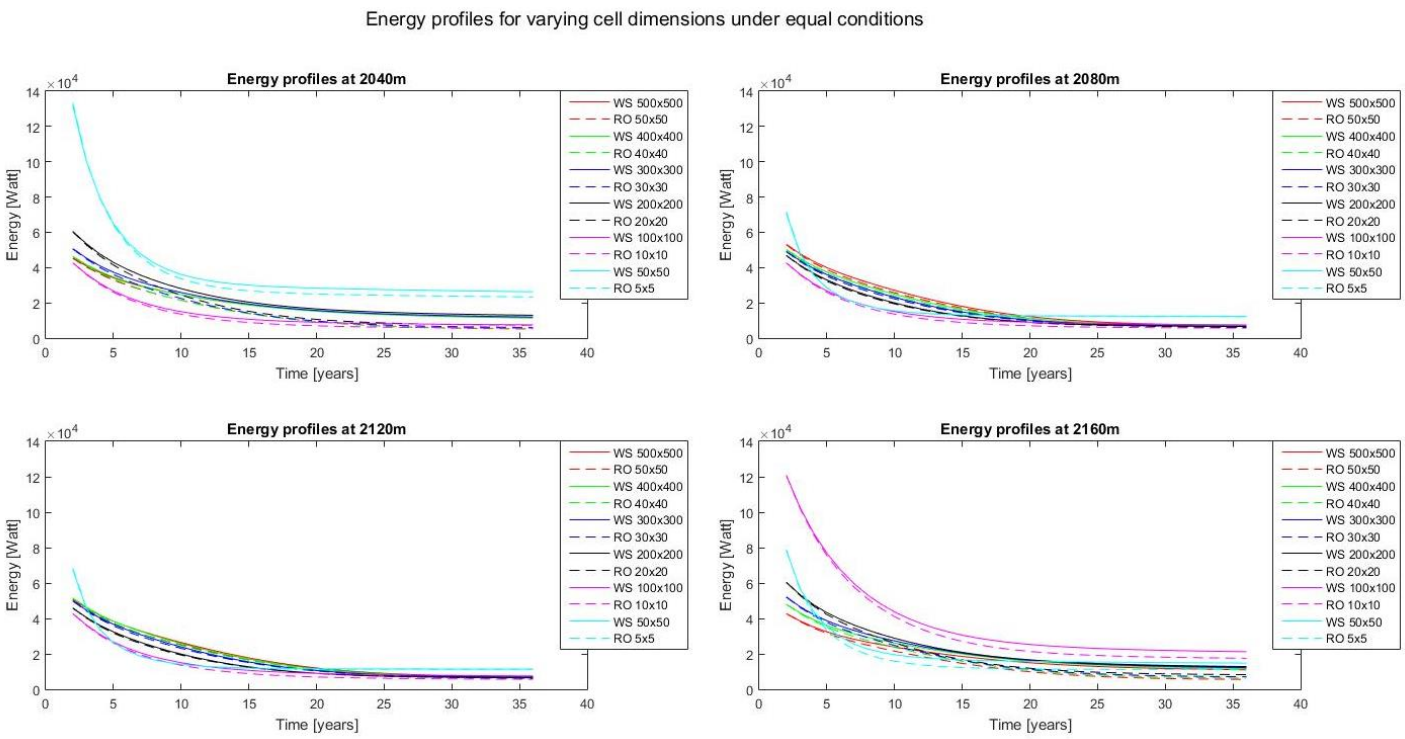

Figure 19: The effect of different cell numbers, and cell dimensions, on simulation results illustrated by thermal energy profiles of a generalised test case. Model dimensions and parameters are kept constant.

Table 8: The number of cells used in the simulation and their resulting cell dimensions.

Number of cells (number of reservoir cells)	Cell dimensions	
	Δy	Δx
500 x 500 (50 x 50	4	20
400 x 400 (40 x 40)	5	25
300 x 300 (30 x 30)	6.67	33.3
200 x 200 (20 x 20)	10	50
100 x 100 (10 x 10)	20	100
50 x 50 (5 x 5)	40	200

The resolution of 200 by 200 cells (Δy = 10 and Δx = 50) applied in the simulations described above corresponds to the lowest possible number of cells without losing simulator stability and without significantly increasing computational time, yet maintaining simulator accuracy. However, a slightly higher accuracy might be preferred at the cost of computational time.

5.1.2. Model dimensions / scale

The simulator used in this study is somewhat limited by the number of cells that can be used in the model domain and only a square grid (a symmetric matrix in the linear system) can be applied. These limitations consequently limit the scale of the model domain. The scale of investigation of the subsurface (geothermal system) used in the simulations, although sufficient, covers a relatively small vertical interval. Preferably, one would investigate a vertical interval of 5 or 6 kilometers, with the top model surface being the actual Earth's surface.

In addition, the dimensions of the model are restricted by reservoir thickness and reservoir length, originating from the fact that the cell dimensions for the reservoir domain must agree with the cell dimensions for the surrounding system domain. For example, when a reservoir has a thickness of 200 m and a length of 1000 m, which is the case in the test cases described above, and a small Δy is applied to

ensure sufficient reservoir cells, the vertical dimension of the surrounding system is limited by the Δy applied to the reservoir cells, thus incorporating a limited vertical interval. The small Δy also results in a much larger Δx to account for the reservoir length, increasing the lateral extent of the model domain significantly. However, a distance of 10 km is preferred since a large distance from each open-hole section to the model boundaries is required to ensure no direct impact of the imposed (lateral) model boundaries (Wanatabe et al., 2017). These limitations are carried with a varying total number of cells used in the model domain. As for the open-hole sections, the fine detail required for modeling flow around wells becomes insignificant when the scale is increased to integrate the geothermal system (Grant & Bixley, 2011).

5.2. Effect of the geothermal system

The results presented in chapter 4 (in particular figure 6 to figure 17) show that the surrounding geothermal system can have a strong influence on the geothermal reservoir. In all cases and for all investigated parameters, the simulations incorporating the geothermal system show (sometimes significantly) higher water temperatures in the production well and increased thermal energy from the production well, compared to the simulations where only the reservoir is considered.
As for convective heat transfer recharge into a geothermal reservoir, recharge of heat by conduction can also (significantly) increase the reservoir lifetime. However, conductive heat transfer has a different effect on reservoir temperatures than convective heat transfer.
Convective recharge of heat from an active circulation system supplies the reservoir with thermal fluids that are heated elsewhere, only to be stored in the reservoir. Conductive heat transfer recharge originates from the heat stored in the various subsurface strata. This heat is extracted from these rocks when it is transferred into water that flows through these rocks, or when heat is transferred from a hot, source area to a colder, sink area in the subsurface.
The two conduction dominated test cases described above show exactly this in the simulations of the geothermal reservoir and surrounding system. Heat is transferred by conduction from the reservoir rocks into the reservoir fluid (water), thus cooling them down. When temperatures in the reservoir rocks are lowered, they, in turn, start to extract heat from the rocks surrounding them and so on. When heat is extracted from the geothermal reservoir, it will start to act as a 'heat sink' to its surroundings, thus cooling them down. The heat extracted from the surrounding system is continuously transferred to the reservoir fluid as long as the temperature of the fluid is lower than that of the rock through which it flows.

This process and its effect are clearly illustrated by the results for the top and bottom perforations in the production well. Water temperatures and thermal energy are significantly higher when the geothermal system in considered. This effect is less significant in the two middle perforations, because of reservoir thickness and the relatively short simulation time. The top and bottom perforations are closer to the strata surrounding the reservoir boundaries and are therefore subjected to a greater conductive heat flux into the reservoir. In addition, when the conductive heat from the surroundings reaches the saturated part of the reservoir (in this case around the depth of the top and bottom perforations), the heat transfer mechanism changes (Benoit, 1978; Salveson & Cooper, 1979, as cited in Grant & Bixley, 2011). So, the center of the reservoir (around the two middle perforations) only experiences heat transfer recharge by convection, originating from the conductive heat transfer from the surroundings, and lowering the effect of the surrounding geothermal system on reservoir lifetime.

In terms of thermal energy production, this phenomenon also applies. The initial thermal energy production from the top and bottom perforations is increased due to an increase in temperature of the reservoir water that is initially present in the top and bottom areas of the reservoir. These waters are heated before production, in the period before the colder (re-)injected water reaches these perforations in the production well.

5.3. Effect of reservoir parameters

The investigated parameters for their effect on geothermal reservoir lifetime are; 1) permeability, 2) porosity, 3) rock thermal conductivity, 4) rock specific heat capacity, 5) injection temperature, and 6) well flow rate, or productivity index. These parameters where investigated in the context of reservoir lifetime; water temperature in the production well and thermal energy extracted from the production well. The results of each parameter will be discussed separately.

5.3.1. Permeability

Permeability has a significant effect on reservoir lifetime in terms of produced water temperatures. The reduction in thermal drawdown can reach values up to %26.5. Exact values generally depend on the specific field parameters. Although the lowest possible water temperature in the production well is still dependent on the (re-)injection temperature, the time required to reach, or approach, this lower temperature limit is strongly dependent on permeability, i.e. the time required for the (re-)injected (cooler) water to reach the production well. The produced water temperatures rapidly decrease (or approach injection temperature) with increasing permeability, as is illustrated by a reduction in thermal drawdown of only %5.9.

There is a clear difference between the temperature profiles for the geothermal system and those for the geothermal reservoir only. This difference decreases as permeability increases, and vice versa, with interdependent differences decreasing from 10.7-13.5 ^{o}C to 3.2-4 ^{o}C.

This can be explained by the time that heat can be transferred from the hot reservoir rocks to the cooler reservoir fluids. As fluids pass through the reservoir rock more quickly, the time that a certain volume of water is in contact with a certain surface area of hot rock is decreased. Assuming the heat transfer coefficient and the temperature difference between fluid and rock on a certain interval in the reservoir are constant, the time it takes for the cooler fluids to reach new thermal equilibrium when in contact with the hot rock on that interval is also constant. Thus, as the time the fluids are in contact with the hot rock on that interval decreases, when permeability increases, the fluids are not able to fully reach new thermal equilibrium with the surrounding hot rock. This not only results in a faster temperature drawdown of produced fluids, it also lowers the effect of the surrounding geothermal system as the fluid temperature does not (or approaches less) the temperature of the new thermal equilibrium.

However, when permeability decreases, the amount of time a volume of fluids is in contact with hot rock on a certain interval in the reservoir starts to approach the amount of time it takes for the fluids to reach new thermal equilibrium relative to the reservoir rock temperature, thus increasing the effect of heat transfer from the geothermal system surrounding the reservoir as the fluid temperature is approaching new thermal equilibrium temperature.

In terms of thermal energy produced from the production well, this phenomenon appears to be reversed. Differences between energy profiles at equal permeability are minimal and may even reduce to zero when the simulation time is increased. From figure 9 and table 4 it becomes clear that the annual average thermal energy produced increases with increasing permeability. Higher permeability results in a higher energy production in the first years of reservoir development, but higher permeability also results in a faster decline of produced energy in these years. Lower permeability gives a more stable energy production rate during reservoir development. The thermal energy production rate is strongly dependent on the flow rate in the reservoir and in the production well, which increases with increasing permeability and although this rate declines more rapidly with higher permeability, it is also maintained at a higher level compared to energy production rates related to lower permeability values.

In terms of the relative increase in annual average thermal energy production, a relatively low permeability value shows the highest increase when the surrounding geothermal system is incorporated, suggesting the existence of an ‘optimal permeability’.

5.3.2. Porosity

Porosity has minimal to no direct effect on reservoir heat extraction lifetime (direct effect, here, excludes its possible contribution to permeability). Differences in thermal drawdown for varying porosities are minimal and differences between simulations with and without consideration of the geothermal system vary only 0.22 and 0.27 ^{o}C for the top and bottom perforations respectively, and 0.2 ^{o}C for the middle perforations. It does however have a small effect on the water temperature during thermal drawdown in the production well. A higher porosity value increases temperatures during thermal drawdown, as a larger body of heated water in the reservoir rock is initially present, at initial reservoir temperatures. This results in higher temperatures of produced waters during development, but also increases the rate of thermal drawdown, as illustrated by the slightly lower reduction in thermal drawdown ratio (table 5). The surrounding geothermal system has an increasing effect on reservoir lifetime for decreasing porosity values, as the reduction in thermal drawdown ratio decreases. The same applies to the thermal energy produced, where the annual average production increases with increasing porosity, but the relative increase in production values, as a result of incorporating the geothermal system, increases with decreasing porosity.

This can be explained by the assumption of only conductive heat transfer recharge from the surrounding system. With increasing porosity, more heat is initially stored in the reservoir fluid and since recharge of heat is dependent on the rocks, the contribution of the surrounding system appears to decrease. However, this is thus only due to the fact that relatively less heat is initially stored in the volume of the reservoir domain consisting of rock. This phenomenon will turn out to be exactly opposite for rock specific heat capacity, and will be discussed in section 5.3.4..

5.3.3. Thermal conductivity

Rock thermal conductivity has a small effect on reservoir heat extraction lifetime in terms of produced water temperature by slightly increasing temperatures in the final stages of reservoir development (after thermal drawdown) when the geothermal system is incorporated in the simulation. Temperature differences after 35 years between simulation models increase with increasing rock thermal conductivity, as well as an increasing ratio of reduction in thermal drawdown up to %22.6. When only the geothermal reservoir is considered in the simulation, rock thermal conductivity appears to have no effect on water temperatures. Considering the geothermal system, increasing values of rock thermal conductivity also increase the difference between temperature profiles at equal conditions with and without consideration of the surrounding system. This effect is much greater in the top and bottom perforations. As described above, heat is transferred mostly by conduction in these parts of the reservoir, while the central part is subject to convective heat transfer. This means that in terms of rock thermal conductivity the contribution of the surrounding system is greater in the top and bottom perforations, as the middle perforations are mostly subjected to convective heat transfer.

Increasing rock thermal conductivity also decreases the rate of thermal drawdown, especially in the top and bottom perforations. Rock thermal conductivity expresses the rate of heat transfer by conduction through the rock, so as heat is extracted from the reservoir rock at a constant rate, the rate of heat transfer from the rocks in the surrounding system into the reservoir rock increases with increasing conductivity, thus increasingly recharging reservoir rock temperature and eventually increasing the produced water temperature.

The same applies to the thermal energy from the production well, with the exception that in terms of energy there is no effect of the surrounding system on the energy profiles for the two middle perforations. Considering the annual average thermal energy production, however, annual production rates increase with increasing rock thermal conductivity. Especially the relative increase in production when considering the geothermal system shows a significantly higher values for increasing rock thermal conductivity.

5.3.4. Specific heat capacity

Rock specific heat capacity has, like porosity, minimal to no effect on reservoir lifetime. Differences in thermal drawdown for varying rock specific heat capacities are minimal and differences between simulations with and without consideration of the geothermal system vary only 0.6 and 0.83 ^{o}C for the top and bottom perforations respectively, and 0.3 ^{o}C for the middle perforations.

The heat initially in place is stored in part in the rock, and in part in the body of water saturating these rocks. The model porosity for test case 2 was fixed at 1%, resulting in a much larger volume of rock in the reservoir domain. As heat capacity is an extensive property of rock, it is proportional to the size of the system, or the volume of rock, resulting in a slightly greater effect (than for porosity) of rock (specific) heat capacity on the produced thermal water temperature. The greater differences during thermal drawdown are a result of the greater variation in investigated parameter values.

The specific heat capacity is used to express the thermal capacity as an intensive property, where the dependency on size or volume, is replaced by mass. Assuming the initial thermal energy in place is kept constant, an increase in specific heat capacity results in a decrease in thermal drawdown because more energy is required for the same drop in temperature of the rocks. This means that the temperature difference between rock and fluid is maintained longer and this, in combination with constant permeability, results in a decrease in thermal drawdown temperatures, or an increase in the ratio of reduction in thermal drawdown with increasing rock specific heat capacity (table 7). Thus, the effect of rock (specific) heat capacity is opposite to the effect of porosity; the surrounding geothermal system has an increasing effect on reservoir lifetime for increasing heat capacity values.

As thermal water temperatures are lowered more slowly, and specific heat capacity is constant, the amount of thermal energy produced also decreases more slowly and thus the annual average thermal energy

produced increases with increasing rock specific heat capacity. However, the relative increase in production values, as a result of incorporating the geothermal system, decreases with increasing heat capacity. This can be explained by the assumption of a constant rock specific heat capacity value throughout the model domain. When heat capacity decreases, the rocks in the surrounding system are less capable of containing heat, therefore more heat is conducted into the reservoir domain, resulting in a greater effect of the surrounding geothermal system.

5.3.5. Injection temperature

The effect of temperature of the (re-)injected water on reservoir lifetime is relatively significant. As mentioned above, the lowest possible water temperature, or maximum drawdown, in the production well is directly dependent on this (re-)injection temperature. Temperatures in the geothermal system, and its reservoir first, will eventually approach the minimum temperature present, i.e. the (re-)injection temperature. Thus, thermal drawdown is decreased with increasing (re-)injected water temperature. This also applies to the produced thermal energy profiles, based on the thermal energy stored in the (re-)injected waters. However, the exact (re-)injection temperature is not reached when only the reservoir is considered in simulations. In this case, for test case 1, the produced water temperature stays about 5 or 6 ^{o}C above (re-)injection temperature, and for test case 2 this is 12 or 13 ^{o}C. These differences are explained by the Neumann boundary condition of constant heat flux at the south model boundary. This boundary condition is applied in simulations for both domains of each test case, or model, and assures that the (re-)injection temperature is not reached, only approached. Furthermore, since the heat flux assumed in test case 2 is more than 2 times the magnitude of the flux assumed in test case 1, the resulting difference between produced temperatures after thermal drawdown and (re-)injection temperatures for both test cases are also different, i.e. difference for test case 2 is more than 2 times as much as for test case 1. This suggests a linear relation between magnitude of the heat flux and the decrease in thermal drawdown.

In addition, the (re-)injected water temperature also plays a significant role in the effect of the surrounding geothermal system on the reservoir lifetime. The differences between the temperature (and energy) profiles for the simulation with and without consideration of the surrounding system start to increase when a lower (re-)injection temperature is considered. Due to the lower (re-)injection temperature, the temperature difference between reservoir and surroundings increases, resulting in an increase in heat transferred into the reservoir. This is illustrated by an increasing ratio of reduction in thermal drawdown with decreasing (re-)injection water temperatures and increasing differences between temperatures at the latest time step considering either reservoir- or geothermal system simulations. Again, this also applies to the thermal energy produced, which increases with increasing (re-)injection temperature, but the relative increase in produced thermal energy increases with decreasing (re-)injection temperature, i.e. the effect of the surrounding geothermal system on reservoir lifetime increases with decreasing (re-)injection temperature.

As the temperature of (re-)injected water is greatly dependent on the thermal extraction process in the surface power plant, this means that more heat could be extracted from produced waters in the surface power plant without water temperatures in the production well dropping below a minimum required for the surface plant application when the surrounding geothermal system is considered, i.e. higher energy production rates while maintaining reservoir lifetime. On the other hand, when energy production rates are kept constant, incorporating the geothermal system in the simulations could greatly extend reservoir lifetime in a low temperature system, such as the one described in test case 2.

6. Conclusion

The aim of this study was to investigate the effect of conductive heat transfer recharge from the surrounding geothermal system, and of multiple reservoir and production parameters, on geothermal reservoir lifetime during development. A non-isothermal lumped-parameter model is assumed for 2 test cases, modelled after existing low temperature, conduction dominated geothermal fields. Resulting produced thermal water temperature and thermal energy flow rate profiles are simulated with and without consideration of the geothermal system.

Results show that the integrated geothermal system has a significant effect on reservoir lifetime by reducing temperatures after thermal drawdown up to %26.5 in test case 1, and up to %22.6 in test case 2, and increasing the average annual thermal energy production up to %12.5 and %14.3, respectively. Based on the studied test cases, permeability, rock thermal conductivity and (re-)injection temperature are the reservoir and production parameters that have the most significant influence on reservoir lifetime.

In conclusion, by integrating the surrounding conduction dominated geothermal system in the simulation of reservoir development, the lifetime of the low temperature reservoir can be greatly increased.

7. Recommendations

In light of future work on simulating geothermal systems, recommendations are given as to where the simulator can be improved to better simulate geothermal reservoir behavior during the development of a geothermal system. The 2D geothermal reservoir simulator (developed mainly by T. Praditia (2017), and modified and extended here for the purpose of this research) is based on a non-isothermal lumped parameter model, assuming both homogeneity and heterogeneity, although on a large scale, and rock and reservoir parameter isotropy. So in general terms, the simulator can be improved by an extension to 3 dimensions, a multiscale model (Praditia, 2017), fine scale heterogeneity and applying rock and reservoir parameter anisotropy. Other important and required improvements in the context of future work are given below.

7.1. Cell dimensions and scale

A big improvement would be to implement the use of different cell dimensions for the reservoir domain and the surrounding system domain. This will allow for the use of sufficient reservoir cells without limiting the vertical dimensions of the surrounding domain, thus increasing the scale of investigation without losing accuracy of the simulation in the reservoir domain. It will also reduce the lateral dimensions of the surrounding domain, while maintaining reservoir length. Another improvement to achieve the latter would be the use of an asymmetric matrix in the linear system of equations, also limiting the lateral extension of the model domain.

7.2. Reservoir thickness and doublet spacing

As discussed in section 5.2., the surrounding geothermal system has the biggest effect on the top and bottom part of the reservoir. Therefore, reservoir thickness might have an influence on the reservoir lifetime, in terms of magnifying the effect of the surrounding geothermal system when a smaller reservoir thickness is assumed or modelled.
Following the study performed by Cees Willems (2017), doublet spacing can also have a significant effect on reservoir lifetime. It will be interesting to study the effect of the surrounding system on the geothermal reservoir, assuming variable doublet spacing. In addition, the number and depths of the perforations in the injection and production well might also be varied.

7.3. Convective heat transfer recharge

A next step in studying the effect of the geothermal system surrounding the reservoir is to implement convective heat transfer recharge, in order to incorporate i.e.; the effect of a thermal aquifer crossing the reservoir, and/or the natural recharge to the reservoir from heated surface waters, depending on their presence in the geologic and hydrologic setting that is modelled.
This way the full capacity of the geothermal system to extend reservoir lifetime can be investigated, as well as a wider variety of geothermal systems and settings.

7.4. Fractures

The main feature of an Enhanced Geothermal System is the creation of permeability by hydraulic fracturing. Test case 2 assumes a constant permeability based on reported fracture permeability, but does not incorporate the explicit influence of fracture aperture and preferential flow paths in the reservoir (Grant & Bixley, 2011; Hajibeygi et al., 2011; Tene et al., 2016; Karvounis & Jenny, 2016). In order to improve the accuracy of simulating an Enhanced Geothermal System, artificial fracturing needs to be implemented in the reservoir domain, in order to study the effect of conductive heat transfer recharge on thermal induced fracture growth (Grant & Bixley, 2011), the effect of increased conductive heat transfer into the fluids occupying the fractures and subsequently the reservoir lifetime.

7.5. Well flow rate

Both the volume of produced thermal waters (mass flow rate) and the amount of produced thermal energy (enthalpy flow rate) are directly dependent on the flow rate in the production well, present or achieved. As the well flow rate increases in the production well, thermal energy is extracted from the reservoir more rapidly, resulting in a faster thermal drawdown (Geothermal production measurement, n.d.). The effect of

flow rate is expected to be much like the effect of permeability discussed above, as flow rate is, in part, dependent on reservoir permeability. Since permeability has a significant effect on reservoir lifetime, it is important to study the effect of flow rates in the production well. These may be increased artificially or due to the presence of fracture dominated permeability. In addition, the energy output of the surface power plant also depends on flow rate (Dickson & Fanelli, 2003). When multiple wells and/or thermal fluid composition (for example CO_2) are considered these flow rates will become of great importance to the energy conversion process in the surface power plant.

7.6. Future investigation

Because permeability has a significant influence on thermal drawdown, conductive heat transfer recharge and thus reservoir lifetime, it is important to implement matrix permeability anisotropy in the simulator, and, when artificial fractures are implemented, the fracture permeability. In addition, well flow rate, and injection temperature and pressure will also start to influence the reservoir lifetime.
To get a more realistic simulation of reservoir lifetime, a loss of water volume due to thermal extraction in the surface power plant has to be assumed in the model.

Bibliography

Coats, K. (1977). Geothermal Reservoir Modelling. *Proceedings of SPE Annual Fall Technical Conference and Exhibition*. doi:10.2523/6892-ms

Daniilidis, A., Doddema, L., & Herber, R. (2016). Risk assessment of the Groningen geothermal potential: From seismic to reservoir uncertainty using a discrete parameter analysis. *Geothermics,64*, 271-288. doi:10.1016/j.geothermics.2016.06.014

Dickson, M. H., & Fanelli, M. (2003). *Geothermal energy: utilization and technology*. Paris, FR: United Nations Educational, Scientific and Cultural Organization (UNESCO).

Dinoloket. (n.d.). Retrieved May 14, 2017, from https://www.dinoloket.nl/ondergrondmodellen

Eppelbaum, L., Kutasov, I., & Pilchin, A. (2014). Applied Geothermics. *Lecture Notes in Earth System Sciences*. doi:10.1007/978-3-642-34023-9

Gehringer, M., & Loksha, V. (2012). *ESMAP Geothermal Handbook: Planning and Financing Power Generation* (Rep.). Washington DC: The World Bank.

geothermal energy. (n.d.). *The American Heritage©New Dictionary of Cultural Literacy, Third Edition.* Retrieved April 14, 2017 from Dictionary.com website http://www.dictionary.com/browse/geothermal-energy

Geothermal production measurement. (n.d.). Retrieved July 13, 2017, from http://petrowiki.org/Geothermal_production_measurement

Grant, M. A., & Bixley, P. F. (2011). Geothermal Reservoir Engineering. *Geothermal Reservoir Engineering*. doi:10.1016/b978-0-12-383880-3.10022-8

Hajibeygi, H., & Jenny, P. (2009). Multiscale finite-volume method for parabolic problems arising from compressible multiphase flow in porous media. *Journal of Computational Physics, 228* (14), 5129-5147. doi:10.1016/j.jcp.2009.04.017

Hajibeygi, H., Karvounis, D.C., Jenny, P. (2011). A hierarchical fracture model for the iterative multiscale finite volume method. *Journal of Computational Physics, 230* (24), 8729-8743.

Harvey, C., & GeothermEx, Inc. (2013). *Geothermal Exploration Best Practices: a guide to resource data collection, analysis, and presentation for geothermal projects* (Publication). Bochum, Germany: IGA Service GmbH.

Karvounis, D.C., & Jenny, P. (2016). Adaptive Hierarchical Fracture Model for Enhanced Geothermal Systems. *Multiscale Modeling and Simulation, 14* (1) 207-231. doi: 10.1137/140983987

Middenmeer, North Holland Monthly Climate Average, Netherlands. (n.d.). Retrieved May 9, 2017, from https://www.worldweatheronline.com/middenmeer-weather-averages/north-holland/nl.aspx

Praditia, T. (2017). *Multiscale finite volume for enhanced geothermal systems*. (Unpublished master thesis). Delft University of Technology.

Pollack, H. N., Hurter, S. J., & Johnson, J. R. (1993). Heat flow from the Earth's interior: Analysis of the global data set. *Reviews of Geophysics,31*(3), 267-280. doi:10.1029/93rg01249

Pribnow, D., & Clauser, C. (2000). Heat and fluid flow at the Soultz Hot Dry Rock system in the Rhine Graben. *Proceedings World Geothermal Congress,* 3835-3840.

Soultz-Sous-Forets, Alsace 14 Day Weather Forecast, France . (n.d.). Retrieved May 9, 2017, from https://www.worldweatheronline.com/soultz-sous-forets-weather/alsace/fr.aspx

Tene, M., Wang, Y., & Hajibeygi, H. (2015). Adaptive algebraic multiscale solver for compressible flow in heterogeneous porous media. *Journal of Computational Physics, 300*, 679-694. doi:10.1016/j.jcp.2015.08.009

Ţene, M., Al Kobaisi, M.S., & Hajibeygi, H. (2016). Algebraic multiscale method for flow in heterogeneous porous media with embedded discrete fractures (F-AMS). *Journal of Computational Physics, 321*, 819-845.

Tester, J.W., Anderson B.J., Batchelor A.S., Blackwell, D.D., Dipippo R., Drake E.M. (eds.) (2006). *The future of geothermal energy impact of Enhanced Geothermal Systems on the United States in the 21st century.* Prepared by the Massachusetts Institute of technology, under Idaho National Laboratory subcontract No. 6300019 for the U.S. Department of energy, Assistant Secretary for Energy Efficiency and Renewable energy, Office of geothermal Technologies. 358 p. (ISBN-10: 0486477711, ISBN-13: 978-0486477718).

Watanabe, N., Blöcher, G., Cacace, M., Held, S., & Kohl, T. (2017). Geoenergy Modeling III. *SpringerBriefs in Energy*. doi:10.1007/978-3-319-46581-4

Willems, C. J. (2017). *Doublet deployment strategies for geothermal Hot Sedimentary Aquifer exploitation* (Unpublished doctoral thesis). Delft University of Technology. doi:10.4233/uuid:2149da75-ca29-4804-8672-549efb004048